

5

Quantum feedback control

5.1 Introduction

In the preceding chapter we introduced quantum trajectories: the evolution of the state of a quantum system conditioned on monitoring its outputs. As discussed in the preface, one of the chief motivations for modelling such evolution is for quantum feedback control. Quantum feedback control can be broadly defined as follows. Consider a detector continuously producing an output, which we will call a current. Feedback is any process whereby a physical mechanism makes the statistics of the present current at a later time depend upon the current at earlier times. Feedback control is feedback that has been engineered for a particular purpose, typically to improve the operation of some device. Quantum feedback control is feedback control that requires some knowledge of quantum mechanics to model. That is, there is some part of the feedback loop that must be treated (at some level of sophistication) as a quantum system. There is no implication that the whole apparatus must be treated quantum mechanically.

The structure of this chapter is as follows. The first quantum feedback experiments (or at least the first experiments specifically identified as such) were done in the mid 1980s by two groups [WJ85a, MY86]. They showed that the photon statistics of a beam of light could be altered by feedback. In Section 5.2 we review such phenomena and give a theoretical description using linearized operator equations. Section 5.3 considers the changes that arise when one allows the measurement to involve nonlinear optical processes. As well as explaining key results in quantum-optical feedback, these sections introduce important concepts for feedback in general, such as stability and robustness, and important applications such as noise reduction. These sections make considerable use of material from Ref. [Wis04].

From Section 5.4 onwards we turn from feedback on continuous fields to feedback on a localized system that is continuously monitored. We give a general description for feedback in such systems and show how, in the Markovian limit, the evolution including the feedback can be described by a new master equation. We formulate our description both in the Schrödinger picture and in the Heisenberg picture, and we discuss an elegant example for which the former description is most useful: protecting a Schrödinger-cat state from decoherence. In Section 5.5 we redevelop these results for the particular case of a

measurement yielding a current with Gaussian white noise, such as homodyne detection. We include the effects of a white-noise (thermal or squeezed) bath. In Section 5.6 we apply this theory for homodyne-based feedback to a very simple family of quantum-optical systems with linear dynamics. We show that, although Markovian feedback can be described without reference to the conditional state, it is the conditional state that determines both the optimal feedback strength and how the feedback performs. In Section 5.7 we discuss a proposed application using (essentially) Markovian feedback to produce deterministic spin-squeezing in an atomic ensemble. Finally, in Section 5.8 we discuss other concepts and other applications of quantum feedback control.

5.2 Feedback with optical beams using linear optics

5.2.1 Linearized theory of photodetection

The history of feedback in quantum optics goes back to the observation of sub-shot-noise fluctuations in an in-loop photocurrent (defined below) in the mid 1980s by two groups [WJ85a, MY86]. A theory of this phenomenon was soon developed by Yamamoto and co-workers [HY86, YIM86] and by Shapiro *et al.* [SSH⁺87]. The central question they were addressing was whether this feedback was producing real squeezing (defined below), a question whose answer is not as straightforward as might be thought. These treatments were based in the Heisenberg picture. They used quantum Langevin equations where necessary to describe the evolution of source operators, but they were primarily interested in the properties of the beams entering the photodetectors, rather than their sources.

The Heisenberg picture is most convenient if (a) one is interested primarily in the properties of the beams and (b) an analytical solution is possible. To obtain analytical results, it is necessary to treat the quantum noise only within a linearized approximation. We begin therefore by giving the linearized theory for photodetection in the Heisenberg picture.

Using the theory from Section 4.7, the operator for the photon flux in a beam at longitudinal position z_1 is

$$\hat{I}(t) = \hat{b}_1^\dagger(t) \hat{b}_1(t), \quad (5.1)$$

where $\hat{b}_1(t) \equiv \hat{b}(z_1, t)$ as defined in Section 3.11. From that section, it should be apparent that it is not sensible to talk about a photodetector for photons of frequency ω_0 that has a response time comparable to or smaller than ω_0^{-1} , but, as long as we are not interested in times comparable to ω_0^{-1} , we can assume that the signal produced by an ideal photodetector at position z_1 is given by Eq. (5.1).

In experiments involving lasers, it is often the case (or at least it is sensible to assume [Mø197]) that $\hat{b}_1(t)$ has a mean amplitude β such that $\beta^2 = \langle \hat{b}_1^\dagger(t) \hat{b}_1(t) \rangle$. Here, without loss of generality, we have taken β to be real. Because point-process noise is often hard to treat analytically, it is common to linearize Eq. (5.1) by approximating it by

$$\hat{I}(t) = \beta^2 + \delta \hat{I}(t) = \beta^2 + \beta \hat{X}_1(t), \quad (5.2)$$

where the amplitude quadrature fluctuation operator

$$\hat{X}_1(t) = \hat{b}_1(t) + \hat{b}_1^\dagger(t) - 2\beta \quad (5.3)$$

is assumed to have zero mean. This approximation is essentially the same as that used in Section 4.4.2 to treat homodyne detection in the large-local-oscillator limit. It assumes that individual photon counts are unimportant, namely that the system fluctuations are evident only in large numbers of detections. This approximation will be valid if the correlations of interest in the system happen on a time-scale long compared with the inverse mean count rate and if the fluctuations are relatively small:

$$\langle \hat{X}_1(t + \tau) \hat{X}_1(t) \rangle \ll \beta^2 \text{ for } \tau \neq 0. \quad (5.4)$$

In all that follows we will consider only stationary stochastic processes, where the two-time correlation functions depend only on the time difference τ . We cannot consider $\tau = 0$ in Eq. (5.4), because the variance diverges due to vacuum fluctuations:¹

$$\lim_{\tau \rightarrow 0} \langle \hat{X}_1(t + \tau) \hat{X}_1(t) \rangle = \lim_{\tau \rightarrow 0} \delta(\tau). \quad (5.5)$$

Note, however, that in this limit the linearized correlation function agrees with that from Eq. (5.1):

$$\lim_{\tau \rightarrow 0} \langle \hat{I}(t) \hat{I}(t + \tau) \rangle = \lim_{\tau \rightarrow 0} \langle \hat{I}(t) \rangle \delta(\tau) = \lim_{\tau \rightarrow 0} \beta^2 \delta(\tau). \quad (5.6)$$

Just as we defined \hat{x} and \hat{y} quadratures for a system in Chapter 4, here it is also useful to define the phase quadrature fluctuation operator

$$\hat{Y}_1(t) = -i\hat{b}_1(t) + i\hat{b}_1^\dagger(t). \quad (5.7)$$

For free fields, where (taking the speed of light to be unity as usual)

$$\hat{b}(z, t + \tau) = \hat{b}(z - \tau, t), \quad (5.8)$$

the canonical commutation relation for the fields at different positions

$$[\hat{b}(z, t), \hat{b}^\dagger(z', t)] = \delta(z - z') \quad (5.9)$$

implies that the quadratures obey the temporal commutation relation

$$[\hat{X}_1(t), \hat{Y}_1(t')] = 2i\delta(t - t'). \quad (5.10)$$

We define the Fourier-transformed operator as follows:

$$\tilde{X}_1(\omega) = \int_{-\infty}^{\infty} dt \hat{X}_1(t) e^{-i\omega t}; \quad (5.11)$$

and similarly for $\tilde{Y}_1(\omega)$. Note that we use a tilde but drop the hat for notational convenience. Then it is simple to show that

$$[\tilde{X}_1(\omega), \tilde{Y}_1(\omega')] = 4\pi i \delta(\omega + \omega'). \quad (5.12)$$

¹ For thermal or squeezed white noise – see Section 4.8.2 – this δ -function singularity is multiplied by a non-unit constant.

For stationary statistics as we are considering, $\langle \hat{X}_1(t) \hat{X}_1(t') \rangle$ is a function of $t - t'$ only. From this it follows that

$$\langle \tilde{X}_1(\omega) \tilde{X}_1(\omega') \rangle \propto \delta(\omega + \omega'). \quad (5.13)$$

Exercise 5.1 Verify Eqs. (5.12) and (5.13).

Because of the singularities in Eqs. (5.12) and (5.13), to obtain a finite uncertainty relation it is more useful to consider the spectrum

$$S_1^X(\omega) = \frac{1}{2\pi} \int_{-\infty}^{\infty} \langle \tilde{X}_1(\omega) \tilde{X}_1(-\omega') \rangle d\omega' \quad (5.14)$$

$$= \int_{-\infty}^{\infty} e^{-i\omega t} \langle \hat{X}_1(t) \hat{X}_1(0) \rangle dt = \langle \tilde{X}_1(\omega) \hat{X}_1(0) \rangle. \quad (5.15)$$

Note that the final expression involves both \hat{X}_1 and \tilde{X}_1 . Equation (5.15) is the same as the spectrum defined for a homodyne measurement of the x quadrature in Section 4.4.4 if we take the system quadrature x to have zero mean. In the present case, the spectrum can be experimentally determined as

$$S_1^X(\omega) = \langle \hat{I}(t) \rangle^{-1} \int_{-\infty}^{\infty} e^{-i\omega t} \langle \hat{I}(t), \hat{I}(0) \rangle dt, \quad (5.16)$$

where $\langle A, B \rangle \equiv \langle AB \rangle - \langle A \rangle \langle B \rangle$ as previously. In fact it is possible to determine $S_1^Q(\omega)$ for any quadrature Q in a similar way by adding a local oscillator of suitable amplitude and phase, as described in Section 4.4.

It can be shown [SSH⁺87] that, for a stationary free field, the commutation relations (5.10) imply that

$$S_1^X(\omega) S_1^Y(\omega) \geq 1. \quad (5.17)$$

This can be regarded as an uncertainty relation for continuum fields. A coherent continuum field where $\hat{b}_1|\beta\rangle = \beta|\beta\rangle$ has, for all ω ,

$$S_1^Q(\omega) = 1, \quad (5.18)$$

where $Q = X$ or Y (or any intermediate quadrature). This is known as the *standard quantum limit* or *shot-noise limit*. A *squeezed* continuum field is one such that, for some ω and some Q ,

$$S_1^Q(\omega) < 1. \quad (5.19)$$

This terminology is appropriate for the same reason as for single-mode squeezed states: the reduced noise in one quadrature gets ‘squeezed’ out into the other quadrature, because of Eq. (5.17).

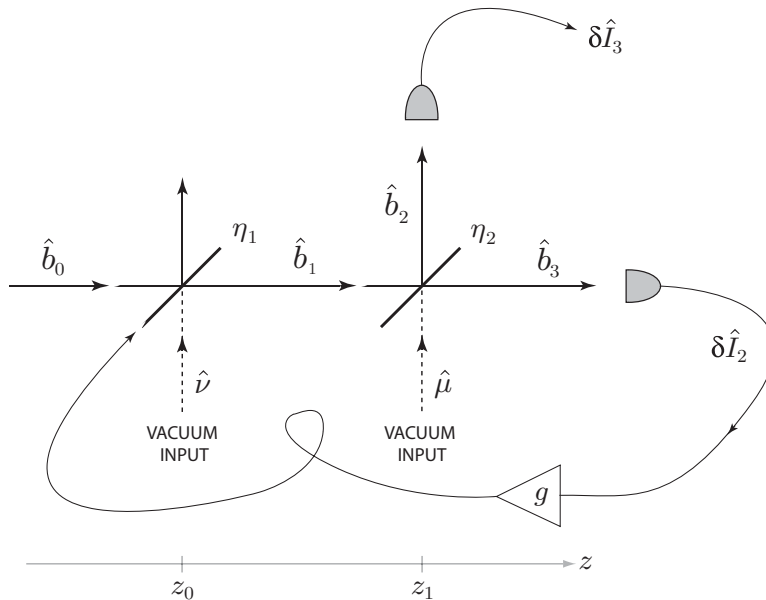


Fig. 5.1 A diagram for a travelling-wave feedback experiment. Travelling fields are denoted \hat{b} and photocurrent fluctuations δI . The first beam-splitter transmittance, η_1 , is variable, the second, η_2 , fixed. The two vacuum field inputs are denoted \hat{v} and $\hat{\mu}$. *Quantum Squeezing*, 2004, pp. 171–122, Chapter 6 ‘Squeezing and Feedback’, H. M. Wiseman, Figure 6.1, Springer-Verlag, Berlin, Heidelberg. Redrawn and revised and adapted with kind permission of Springer Science+Business Media.

5.2.2 In-loop ‘squeezing’

The simplest form of quantum optical feedback is shown in Fig. 5.1. This was the scheme considered by Shapiro *et al.* [SSH⁺87]. In our notation, we begin with a field $\hat{b}_0 = \hat{b}(z_0, t)$ as shown in Fig. 5.1. We will take this field to have stationary statistics with mean amplitude β and fluctuations

$$\frac{1}{2}[\hat{X}_0(t) + i\hat{Y}_0(t)] = \hat{b}_0(t) - \beta. \quad (5.20)$$

We take the amplitude and phase noises to be independent and characterized by arbitrary spectra $S_0^X(\omega)$ and $S_0^Y(\omega)$, respectively.

This field is then passed through a beam-splitter of transmittance $\eta_1(t)$. By unitarity, the diminution in the transmitted field by a factor $\sqrt{\eta_1(t)}$ must be accompanied by the addition of vacuum noise from the other port of the beam-splitter (see Section 4.4.1). The transmitted field is

$$\hat{b}_1(t) = \sqrt{\eta_1(t - \tau_1)} \hat{b}_0(t - \tau_1) + \sqrt{\bar{\eta}_1(t - \tau_1)} \hat{v}(t - \tau_1). \quad (5.21)$$

Here $\tau_1 = z_1 - z_0$ and we are using the notation

$$\bar{\eta}_j \equiv 1 - \eta_j. \quad (5.22)$$

The annihilation operator $\hat{v}(t)$ represents the vacuum fluctuations. The vacuum is a special case of a coherent continuum field of vanishing mean amplitude $\langle \hat{v}(t) \rangle = 0$, and so is completely characterized by its spectrum

$$S_v^Q(\omega) = 1. \quad (5.23)$$

Since the vacuum fluctuations are uncorrelated with any other field, and have stationary statistics, the time argument for $\hat{v}(t)$ is arbitrary (when it first appears).

The beam-splitter transmittance $\eta_1(t)$ in Eq. (5.21) is time-dependent. This time-dependence can be achieved experimentally by a number of means. For example, if the incoming beam is elliptically polarized then an electro-optic modulator (a device with a refractive index controlled by a current) will alter the orientation of the ellipse. A polarization-sensitive beam-splitter will then control the amount of the light which is transmitted, as done, for example, in [TWMB95]. As the reader will no doubt have anticipated, the current used to control the electro-optic modulator can be derived from a later detection of the light beam, giving rise to feedback. Writing $\eta_1(t) = \bar{\eta}_1 + \delta\eta_1(t)$, and assuming that the modulation of the transmittance is small ($\delta\eta_1(t) \ll \bar{\eta}_1$), one can write

$$\sqrt{\eta_1(t)} = \sqrt{\bar{\eta}_1} + (1/\sqrt{\bar{\eta}_1})^{1/2} \delta\eta_1(t). \quad (5.24)$$

Continuing to follow the path of the beam in Fig. 5.1, it now enters a second beam-splitter of constant transmittance η_2 . The transmitted beam annihilation operator is

$$\hat{b}_2(t) = \sqrt{\eta_2} \hat{b}_1(t - \tau_2) + \sqrt{\bar{\eta}_2} \hat{\mu}(t - \tau_2), \quad (5.25)$$

where $\tau_2 = z_2 - z_1$ and $\hat{\mu}(t)$ represents vacuum fluctuations like $\hat{v}(t)$. The reflected beam operator is

$$\hat{b}_3(t) = \sqrt{\bar{\eta}_2} \hat{b}_1(t - \tau_2) - \sqrt{\eta_2} \hat{\mu}(t - \tau_2). \quad (5.26)$$

Using the approximation (5.24), the linearized quadrature fluctuation operators for \hat{b}_2 are

$$\begin{aligned} \hat{X}_2(t) &= \sqrt{\eta_2 \bar{\eta}_1} \hat{X}_0(t - T_2) + \sqrt{\eta_2 / \bar{\eta}_1} \beta \delta\eta_1(t - T_2) \\ &\quad + \sqrt{\eta_2 \bar{\eta}_1} \hat{X}_v(t - T_2) + \sqrt{\bar{\eta}_2} \hat{X}_\mu(t - T_2), \end{aligned} \quad (5.27)$$

$$\begin{aligned} \hat{Y}_2(t) &= \sqrt{\eta_2 \bar{\eta}_1} \hat{Y}_0(t - T_2) \\ &\quad + \sqrt{\eta_2 \bar{\eta}_1} \hat{Y}_v(t - T_2) + \sqrt{\bar{\eta}_2} \hat{Y}_\mu(t - T_2), \end{aligned} \quad (5.28)$$

where $T_2 = \tau_2 + \tau_1$. Here, for simplicity, we have shifted the time argument of the μ vacuum quadrature operators by τ_1 . This is permissible because the vacuum noise is a stationary process (regardless of any other noise processes). Similarly, for \hat{b}_3 we have

$$\begin{aligned} \hat{X}_3(t) &= \sqrt{\bar{\eta}_2 \bar{\eta}_1} \hat{X}_0(t - T_2) + \sqrt{\bar{\eta}_2 / \bar{\eta}_1} \beta \delta\eta_1(t - T_2) \\ &\quad + \sqrt{\bar{\eta}_2 \bar{\eta}_1} \hat{X}_v(t - T_2) - \sqrt{\eta_2} \hat{X}_\mu(t - T_2), \end{aligned} \quad (5.29)$$

$$\begin{aligned} \hat{Y}_3(t) &= \sqrt{\bar{\eta}_2 \bar{\eta}_1} \hat{Y}_0(t - T_2) + \sqrt{\bar{\eta}_2 \bar{\eta}_1} \hat{Y}_v(t - T_2) \\ &\quad - \sqrt{\eta_2} \hat{Y}_\mu(t - T_2). \end{aligned} \quad (5.30)$$

Exercise 5.2 *Derive Eqs. (5.27)–(5.30).*

The mean fields for \hat{b}_2 and \hat{b}_3 are $\sqrt{\eta_1\eta_2}\beta$ and $\sqrt{\eta_1\bar{\eta}_2}\beta$, respectively. Thus, if these fields are incident upon photodetectors, the respective linearized photocurrent fluctuations are, as explained in Section 5.2.1,

$$\delta\hat{I}_2(t) = \sqrt{\eta_1\eta_2}\beta\hat{X}_2(t), \quad (5.31)$$

$$\delta\hat{I}_3(t) = \sqrt{\eta_1\bar{\eta}_2}\beta\hat{X}_3(t). \quad (5.32)$$

Here we have assumed perfect-efficiency detectors. Inefficient detectors can be modelled by further beam-splitters (see Section 4.8), and the effect of this has been considered in detail in Refs. [MPV94, TWMB95].

Having obtained an expression for $\delta\hat{I}_2(t)$, we are now in a position to follow the next stage in Fig. 5.1 and complete the feedback loop. We set the modulation in the transmittance of the first beam-splitter to be

$$\delta\hat{\eta}_1(t) = \frac{g}{\eta_2\beta^2} \int_0^\infty h(t')\delta\hat{I}_2(t - \tau_0 - t')dt', \quad (5.33)$$

where g is a dimensionless parameter. It represents the low-frequency gain of the feedback, as will be seen. The response of the feedback loop, including the electro-optic elements, is assumed to be linear for small fluctuations and is characterized by the electronic delay time τ_0 and the response function $h(t')$, which satisfies $h(t) = 0$ for $t < 0$, $h(t) \geq 0$ for $t > 0$ and $\int_0^\infty h(t')dt' = 1$.

The appearance of a hat on the beam-splitter transmittance η_1 in Eq. (5.33) may give the impression that one is giving a quantum-mechanical treatment of a macroscopic system. This is a false impression. The only features of the operators which are important are their stochastic nature and their correlations with the source. The macroscopic apparatus has not been quantized; it is simply correlated to the fluctuations in the observed photocurrent, which are represented by an operator, as explained in Sections 1.3 and 4.7. In the quantum trajectory description of feedback, which is considered in the later sections of this chapter, this false impression would never arise. The feedback apparatus is treated as a completely classical system, which is of course how experimentalists would naturally regard it.

5.2.3 Stability

Clearly the feedback can affect only the amplitude quadrature \hat{X} . Putting Eq. (5.33) into Eq. (5.27) yields

$$\begin{aligned} \hat{X}_2(t) = & \sqrt{\eta_2\eta_1}\hat{X}_0(t - T_2) + g \int_0^\infty h(t')\hat{X}_2(t - T - t')dt' \\ & + \sqrt{\eta_2\bar{\eta}_1}\hat{X}_v(t - T_2) + \sqrt{\eta_2}\hat{X}_\mu(t - T_2), \end{aligned} \quad (5.34)$$

where $T = \tau_0 + T_2 = \tau_0 + \tau_1 + \tau_2$. This is easy to solve in Fourier space, provided that \hat{X}_2 is a stationary stochastic process. This will be the case if and only if the feedback loop is stable.

The problem of stability in feedback loops is a difficult one in general. However, for a simple linear system such as we are considering here, there are criteria for testing whether a given loop is stable and techniques for designing loops that will satisfy these criteria. For the interested reader, an elementary introduction can be found in Ref. [SSW90]. Here we will not cover this theory in detail, but give only the bare essentials needed for this case. Our aim is to acquire some insight into the stability criteria, and especially the trade-off among the bandwidth of the loop, its gain and the time delay.

We begin by writing Eq. (5.34) in the form

$$\hat{X}_2(t) - g \int_0^\infty h(t') \hat{X}_2(t - T - t') dt' = \hat{f}(t), \quad (5.35)$$

where $\hat{f}(t)$ represents all of the (stationary) noise processes in Eq. (5.34). Now the solution to this equation can be found by taking the Laplace transform:

$$[1 - g h^L(s) \exp(-sT)] \hat{X}_2^L(s) = \hat{f}^L(s), \quad (5.36)$$

where $h^L(s) = \int_0^\infty dt e^{-st} h(t)$ etc.

Exercise 5.3 Derive Eq. (5.36) and show that the low-frequency ($s = 0$) equation is

$$\hat{X}_2^L(0) = g \hat{X}_2^L(0) + \hat{f}^L(0), \quad (5.37)$$

which shows that g is indeed the low-frequency gain of the feedback.

A stable feedback loop means that, for a spectral-bounded noise input $\hat{f}(t)$, the solution $\hat{X}(t)$ will also be spectral-bounded for all times. (Here by ‘spectral-bounded’ we mean that the spectrum, as defined in Eq. (5.14), is bounded from above.) This will be the case if and only if

$$\text{Re}[s] < 0, \quad (5.38)$$

where s is any solution of the characteristic equation

$$1 - g h^L(s) \exp(-sT) = 0. \quad (5.39)$$

This is known as the Nyquist stability criterion [SSW90].

First we show that a *sufficient* condition for stability is $|g| < 1$. Looking for instability, assume that $\text{Re}[s] > 0$. Then

$$|h^L(s) e^{-sT}| = \left| \int_0^\infty dt e^{-s(t+T)} h(t) \right| < \int_0^\infty dt h(t) = 1. \quad (5.40)$$

Thus under this assumption the characteristic equation cannot be satisfied for $|g| < 1$. That is, the $|g| < 1$ regime will always be stable. On the other hand, if $g > 1$ then there is an s with a positive real part that will solve Eq. (5.39).

Box 5.1 The feedback gain–bandwidth relation

Consider feedback as described in the text with the simple smoothing function $h(t) = \Gamma e^{-\Gamma t}$ for $t > 0$. In this case the characteristic equation (5.39) becomes (for g negative)

$$s + \Gamma + |g|\Gamma e^{-sT} = 0. \quad (5.41)$$

On setting $s = T^{-1}(\lambda + i\omega)$ for λ and ω real, and defining $\gamma = \Gamma T$, this is equivalent to the following equations in real, dimensionless variables:

$$\lambda + \gamma = -|g|\gamma e^{-\lambda} \cos \omega, \quad (5.42)$$

$$\omega = +|g|\gamma e^{-\lambda} \sin \omega. \quad (5.43)$$

By combining these equations, one finds the following relation:

$$\lambda = -\gamma - \omega \cot \omega. \quad (5.44)$$

Thus, as long as $\omega \cot \omega$ is positive, the real part of s (that is, $T^{-1}\lambda$) will be negative, as is required for stability. Substituting Eq. (5.44) into Eq. (5.42) or Eq. (5.43) to eliminate λ yields

$$\frac{\omega}{\sin \omega} = |g|\gamma e^{\gamma} e^{\omega \cot \omega}. \quad (5.45)$$

This has no analytical solution, but as long as

$$|g|\gamma e^{\gamma} \leq \pi/2 \quad (5.46)$$

all solutions of this equation satisfy $n\pi \leq |\omega| \leq (n + 1/2)\pi$, for n an integer, and so guarantee that $\omega \cot \omega$ is positive. Moreover, for large gain $|g|$, if $|g|\gamma e^{\gamma}$ is significantly larger than $\pi/2$ then there exist solutions ω to Eq. (5.45) such that λ in Eq. (5.44) is positive.

Thus we have a stability condition (Eq. (5.46)) that is sufficient and, for large feedback gain, not too far from necessary. Since $|g| \gg 1$ requires $\gamma \ll 1$, in this regime the condition simplifies to $|g|\gamma \leq \pi/2$. Returning to the original variables, we thus have the following approximate gain–bandwidth relation:

$$\Gamma \lesssim \frac{\pi}{2T|g|} \ll T^{-1}. \quad (5.47)$$

That is, a finite delay time T and large negative feedback $-g \gg 1$ puts an upper bound on the bandwidth $B = 2\Gamma$ of the feedback (here defined as the full-width at half-maximum height of $|\tilde{h}(\omega)|^2$). Moreover, this upper bound implies that in the average signal delay in the feedback loop, $\int_T^\infty h(\tau)\tau \, d\tau = \Gamma^{-1} + T$, the response-function decay time Γ^{-1} dominates over the raw delay time T .

Exercise 5.4 Prove this by considering the left-hand side of Eq. (5.39) as a function of s on the interval $[0, \infty)$ on the real line. In particular, consider its value at 0 and its value at ∞ .

Thus it is a *necessary* condition to have $g < 1$. If $g < -1$, the stability of the feedback depends on T and the shape of $h(t)$. However, it turns out that it is possible to have arbitrarily large negative low-frequency feedback (that is, $-g \gg 1$), for any feedback loop delay T , provided that $h(t)$ is broad enough. That is, the price to be paid for strong low-frequency negative feedback is a reduction in the bandwidth of the feedback, namely the width of $|\tilde{h}(\omega)|^2$. A simple example of this is considered in Box 5.1, to which the following exercise pertains.

Exercise 5.5 Convince yourself of the statements following Eq. (5.46) by graphing both sides of Eq. (5.45) for different values of $|g|\gamma e^\gamma$.

5.2.4 In-loop and out-of-loop spectra

Assuming, then, that the feedback is stable, we can solve Eq. (5.34) for \hat{X}_2 in the Fourier domain:

$$\tilde{X}_2(\omega) = \exp(-i\omega T_2) \frac{\sqrt{\eta_2 \bar{\eta}_1} \tilde{X}_0(\omega) + \sqrt{\eta_2 \bar{\eta}_1} \tilde{X}_v(\omega) + \sqrt{\bar{\eta}_2} \tilde{X}_\mu(\omega)}{1 - g \tilde{h}(\omega) \exp(-i\omega T)}. \quad (5.48)$$

From this the in-loop amplitude quadrature spectrum is easily found from Eqs. (5.13) and (5.14) to be

$$\begin{aligned} S_2^X(\omega) &= \frac{\eta_1 \eta_2 S_0^X(\omega) + \eta_2 \bar{\eta}_1 S_v^X(\omega) + \bar{\eta}_2 S_\mu^X(\omega)}{|1 - g \tilde{h}(\omega) \exp(-i\omega T)|^2} \\ &= \frac{1 + \eta_1 \eta_2 [S_0^X(\omega) - 1]}{|1 - g \tilde{h}(\omega) \exp(-i\omega T)|^2}. \end{aligned} \quad (5.49)$$

Exercise 5.6 Derive these results.

From these formulae the effect of feedback is obvious: it multiplies the amplitude quadrature spectrum at a given frequency by the factor $|1 - g \tilde{h}(\omega) \exp(-i\omega T)|^{-2}$. At low frequencies, this factor is simply $(1 - g)^{-2}$, which is why the feedback was classified on this basis into positive ($g > 0$) and negative ($g < 0$) feedback. The former will increase the noise at low frequency and the latter will decrease it. However, at higher frequencies, and in particular at integer multiples of π/T , the sign of the feedback will reverse and $g < 0$ will result in an increase in noise and vice versa. All of these results make perfect sense in the context of classical light signals, except that classically we would not worry about vacuum noise. Ignoring the vacuum noise is equivalent to assuming that the noise in the input beam is far above the shot-noise limit, so that one can replace $1 + \eta_1 \eta_2 [S_0^X(\omega) - 1]$ by $\eta_1 \eta_2 S_0^X(\omega)$. This gives the result expected from classical signal processing: the signal is attenuated by the beam-splitters and either amplified or suppressed by the feedback.

The most dramatic effect is, of course, for large negative feedback. For sufficiently large $-g$ it is clear that one can make

$$S_2^X(\omega) < 1 \quad (5.50)$$

for some ω . This effect has been observed experimentally many times with different systems involving feedback; see for example Refs. [WJ85a, MY86, YIM86, MPV94, TWMB95]. Without a feedback loop this sub-shot-noise photocurrent would be seen as evidence for squeezing. However, there are several reasons to be very cautious about applying the description squeezing to this phenomenon relating to the in-loop field. Two of these reasons are theoretical, and are discussed in the following two subsections. The more practical reason relates to the out-of-loop beam \hat{b}_3 .

From Eq. (5.29), the X quadrature of the beam \hat{b}_3 is, in the Fourier domain,

$$\begin{aligned} \tilde{X}_3(\omega) = & \exp(-i\omega T_2) [\sqrt{\bar{\eta}_2 \eta_1} \tilde{X}_0(\omega) + \sqrt{\bar{\eta}_2 \bar{\eta}_1} \tilde{X}_v(\omega) - \sqrt{\eta_2} \tilde{X}_\mu(\omega)] \\ & + \sqrt{\bar{\eta}_2 / \eta_2} g \tilde{h}(\omega) \exp(-i\omega T) \tilde{X}_2(\omega). \end{aligned} \quad (5.51)$$

Here we have substituted for $\delta\eta_1$ in terms of \hat{X}_2 . Now using the above expression (5.48) gives

$$\begin{aligned} \tilde{X}_3(\omega) = & \exp(-i\omega T_2) \left\{ \frac{\sqrt{\bar{\eta}_2 \eta_1} \tilde{X}_0(\omega) + \sqrt{\bar{\eta}_2 \bar{\eta}_1} \tilde{X}_v(\omega)}{1 - g \tilde{h}(\omega) \exp(-i\omega T)} \right. \\ & \left. - \frac{\sqrt{\eta_2} [1 - g \tilde{h}(\omega) \exp(-i\omega T) / \eta_2] \tilde{X}_\mu(\omega)}{1 - g \tilde{h}(\omega) \exp(-i\omega T)} \right\}. \end{aligned} \quad (5.52)$$

This yields the spectrum

$$\begin{aligned} S_3^X(\omega) = & \frac{1 + \bar{\eta}_2 \eta_1 [S_0^X(\omega) - 1]}{|1 - g \tilde{h}(\omega) \exp(-i\omega T)|^2} \\ & + \frac{-2 \operatorname{Re}[g \tilde{h}(\omega) \exp(-i\omega T)] + g^2 |\tilde{h}(\omega)|^2 / \eta_2}{|1 - g \tilde{h}(\omega) \exp(-i\omega T)|^2}. \end{aligned} \quad (5.53)$$

The denominators are identical to those in the in-loop case, as is the numerator in the first line, but the additional term in the numerator of the second line indicates that there is extra noise in the out-of-loop signal.

The expression (5.53) can be rewritten as

$$S_3^X(\omega) = 1 + \frac{\bar{\eta}_2 \eta_1 [S_0^X(\omega) - 1] + g^2 |\tilde{h}(\omega)|^2 \bar{\eta}_2 / \eta_2}{|1 - g \tilde{h}(\omega) \exp(-i\omega T)|^2}. \quad (5.54)$$

From this it is apparent that, unless the initial beam is amplitude-squeezed (that is, unless $S_0^X(\omega) < 1$ for some ω), the out-of-loop spectrum will always be greater than the shot-noise limit of unity. In other words, it is not possible to extract the apparent squeezing in the feedback loop by using a beam-splitter. In fact, in the limit of large negative feedback

(which gives the greatest noise reduction in the in-loop signal), the low-frequency out-of-loop amplitude spectrum approaches a constant. That is,

$$\lim_{g \rightarrow -\infty} S_3^X(0) = \eta_2^{-1}. \quad (5.55)$$

Thus the more light one attempts to extract from the feedback loop, the higher above shot noise the spectrum becomes. Indeed, this holds for any frequency such that $\tilde{h}(\omega) \neq 0$, but recall that for large $|g|$ the bandwidth of $|\tilde{h}(\omega)|^2$ must go to zero (see Box. 5.1).

This result is counter to an intuition based on classical light signals, for which the effect of a beam-splitter is simply to split a beam in such a way that both outputs would have the same statistics. The reason why this intuition fails is precisely because this is not all that a beam-splitter does; it also introduces vacuum noise, which is *anticorrelated* at the two output ports. The detector for beam \hat{b}_2 measures the amplitude fluctuations \hat{X}_2 , which are a combination of the initial fluctuations \hat{X}_0 and the two vacuum fluctuations \hat{X}_v and \hat{X}_μ . The first two of these are common to the beam \hat{b}_3 , but the last, \hat{X}_μ , appears with opposite sign in \hat{X}_3 . As the negative feedback is turned up, the first two components are successfully suppressed, but the last is actually amplified.

5.2.5 Commutation relations

Under normal circumstances (without a feedback loop) one would expect a sub-shot-noise amplitude spectrum to imply a super-shot-noise phase spectrum. However, that is not what is found from the theory presented here. Rather, the in-loop phase quadrature spectrum is unaffected by the feedback, being equal to

$$S_2^Y(\omega) = 1 + \eta_1 \eta_2 [S_0^Y(\omega) - 1]. \quad (5.56)$$

It is impossible to measure this spectrum without disturbing the feedback loop because all of the light in the \hat{b}_2 beam must be incident upon the photodetector in order to measure \hat{X}_2 . However, it is possible to measure the phase-quadrature of the out-of-loop beam by homodyne detection. This was done in [TWMB95], which verified that this quadrature is also unaffected by the feedback, with

$$S_3^Y(\omega) = 1 + \eta_1 \bar{\eta}_2 [S_0^Y(\omega) - 1]. \quad (5.57)$$

For simplicity, consider the case in which the initial beam is coherent with $S_0^X(\omega) = S_0^Y(\omega) = 1$. Then $S_2^Y(\omega) = 1$ and

$$S_2^Y(\omega) S_2^X(\omega) = |1 - g \tilde{h}(\omega) \exp(-i\omega T)|^{-2}. \quad (5.58)$$

This can clearly be less than unity. This represents a violation of the uncertainty relation (5.17) which follows from the commutation relations (5.12). In fact it is easy to show (as done first by Shapiro *et al.* [SSH⁺87]) from the solution (5.48) that the commutation

relations (5.12) are false for the field \hat{b}_2 and must be replaced by

$$[\tilde{X}_2(\omega), \tilde{Y}_2(\omega')] = \frac{4\pi i \delta(\omega + \omega')}{1 - g\tilde{h}(\omega)\exp(-i\omega T)}, \quad (5.59)$$

which explains how Eq. (5.58) is possible.

At first sight, this apparent violation of the canonical commutation relations would seem to be a major problem of this theory. In fact, there are no violations of the canonical commutation relations. As emphasized in Section 5.2.1, the canonical commutation relations (5.9) are between fields at different points in space, *at the same time*. It is only for free fields (travelling forwards in space for an indefinite time) that one can replace the space difference z by a time difference $t = z$ (remember that we are setting the speed of light $c = 1$). Field \hat{b}_3 is such a free field, since it can be detected an arbitrarily large distance away from the apparatus. Thus its quadratures at a particular point do obey the two-time commutation relations (5.10) and the corresponding Fourier-domain relations (5.12). But the field \hat{b}_2 cannot travel an indefinite distance before being detected. The time from the second beam-splitter to the detector τ_2 is a physical parameter in the feedback system.

For time differences shorter than the total feedback loop delay T it can be shown that the usual commutation relations hold:

$$[\hat{X}_2(t), \hat{Y}_2(t')] = 2i\delta(t - t') \quad \text{for } |t - t'| < T. \quad (5.60)$$

The field \hat{b}_2 is only in existence for a time τ_2 before it is detected. Because $\tau_2 < T$, this means that the two-time commutation relations between different parts of field \hat{b}_2 are actually preserved for any time such that those parts of the field are in existence, travelling through space towards the detector. It is only at times greater than the feedback loop delay time T that non-standard commutation relations hold. To summarize, the commutation relations between any of the fields at different spatial points always hold, but there is no reason to expect the time or frequency commutation relations to hold for an in-loop field. Without these relations, it is not clear how ‘squeezing’ should be defined. Indeed, it has been suggested [BGS⁺99] that ‘squashing’ would be a more appropriate term for in-loop ‘squeezing’ because the uncertainty has actually been squashed, rather than squeezed out of one quadrature and into another.

A second theoretical reason against the use of the word squeezing to describe the sub-shot-noise in-loop amplitude quadrature is that (provided that beam \hat{b}_0 is not squeezed), the entire apparatus can be described semiclassically. In a semiclassical description there is no noise except classical noise in the field amplitudes, and shot noise is a result of a quantum detector being driven by a classical beam of light. That such a description exists might seem surprising, given the importance of vacuum fluctuations in the explanation of the spectra in Section 5.2.4. However, the semiclassical explanation, as discussed for example in Refs. [SSH⁺87] and [TWMB95], is at least as simple. Nevertheless, this theory is less general than the quantum theory (it cannot treat an initial squeezed beam) so we do not develop it here.

5.2.6 QND measurements of in-loop beams

The existence of a semiclassical theory as just mentioned suggests that all of the calculations of noise spectra made above relate only to the noise of photocurrents and say nothing about the noise properties of the light beams themselves. However, this is not really true, as can be seen from considering quantum non-demolition (QND) measurements. In QND measurements, the measured observable (one quadrature in this case) is unchanged by the measurement, unlike in an ordinary absorptive measurement in optics. QND measurements cannot be described by semiclassical theory, which again shows that this theory is not complete.

A specific model for a QND device will be considered in Section 5.3.1. Here we simply assume that a perfect QND device can measure the amplitude quadrature X of a continuum field without disturbing it beyond the necessary back-action from the Heisenberg uncertainty principle. In other words, the QND device should give a readout at time t that can be represented by the operator $\hat{X}(t)$. The correlations of this readout will thus reproduce the correlations of $\hat{X}(t)$. For a perfect QND measurement of \hat{X}_2 and \hat{X}_3 , the spectrum will reproduce those of the conventional (demolition) photodetectors which measure these beams. This confirms that these detectors (assumed perfect) are indeed recording the true quantum fluctuations of the light impinging upon them.

What is more interesting is to consider a QND measurement on \hat{X}_1 . That is because the set-up in Fig. 5.1 is equivalent (as mentioned above) to a set-up without the second beam-splitter, but instead with an in-loop photodetector with efficiency η_2 . In this version, the beams \hat{b}_2 and \hat{b}_3 do not physically exist. Rather, \hat{b}_1 is the in-loop beam and \hat{X}_2 is the operator for the noise in the photocurrent produced by the detector. As shown above, \hat{X}_2 can have vanishing noise at low frequencies for $g \rightarrow -\infty$. However, this is not reflected in the noise in the in-loop beam, as recorded by our hypothetical QND device. Following the methods of Section 5.2.4, the spectrum of \hat{X}_1 is

$$S_1^X(\omega) = \frac{1 + \eta_1[S_0(\omega) - 1] + g^2|\tilde{h}(\omega)|^2\bar{\eta}_2/\eta_2}{|1 - g\tilde{h}(\omega)\exp(-i\omega T)|^2}. \quad (5.61)$$

In the limit $g \rightarrow -\infty$, this becomes at low frequencies

$$S_1^X(0) \rightarrow \frac{1 - \eta_2}{\eta_2}, \quad (5.62)$$

which is not zero for any detection efficiency η_2 less than unity. Indeed, for $\eta_2 < 0.5$ it is above shot noise.

The reason why the in-loop amplitude quadrature spectrum is not reduced to zero for large negative feedback is that the feedback loop is feeding back noise $\hat{X}_\mu(t)$ in the photocurrent fluctuation operator $\hat{X}_2(t)$ that is independent of the fluctuations in the amplitude quadrature $\hat{X}_1(t)$ of the in-loop light. The smaller η_2 , the larger the amount of extraneous noise in the photocurrent and the larger the noise introduced into the in-loop light. In order to minimize the low-frequency noise in the in-loop light, there is an optimal feedback gain.

In the case $S_0(\omega) = 1$ (a coherent input), this is given by

$$g_{\text{opt}} = -\frac{\eta_2}{1 - \eta_2}, \quad (5.63)$$

giving a minimum in-loop low-frequency noise spectrum

$$S_1^X(0)|_{g=g_{\text{opt}}} = 1 - \eta_2. \quad (5.64)$$

The fact that the detection efficiency does matter in the attainable squashing (in-loop squeezing) shows that these are true quantum fluctuations.

5.2.7 Applications to noise reduction

Although the feedback device discussed in this section cannot produce a free squeezed beam, it is nevertheless useful for reducing classical noise in the output beam \hat{b}_3 . It is easy to verify the result of [TWMB95] that, if one wishes to reduce classical noise $S_3^X(\omega) - 1$ at a particular frequency ω , then the optimal feedback is such that

$$g\tilde{h}(\omega)\exp(-i\omega T) = -\eta_1\eta_2[S_0^X(\omega) - 1]. \quad (5.65)$$

This gives the lowest noise level in the amplitude of \hat{b}_3 at that frequency,

$$S_3^X(\omega)_{\text{opt}} = 1 + \frac{\bar{\eta}_2\eta_1[S_0^X(\omega) - 1]}{1 + \eta_2\eta_1[S_0^X(\omega) - 1]}. \quad (5.66)$$

For large classical noise we have feedback proportional to $S_0^X(\omega)$ and an optimal noise value of $1/\eta_2$, as this approaches the limit of Eq. (5.55). The interesting regime [TWMB95] is the opposite one, where $S_0^X(\omega) - 1$ is small, or even negative. The case of $S_0^X(\omega) - 1 < 0$ corresponds to a squeezed input beam. Putting squeezing through a beam-splitter reduces the squeezing in both output beams. In this case, with no feedback the residual squeezing in beam \hat{b}_3 would be

$$S_3^X(\omega)|_{g=0} = 1 + \bar{\eta}_2\eta_1[S_0^X(\omega) - 1], \quad (5.67)$$

which is closer to unity than $S_0^X(\omega)$. The optimal feedback (the purpose of which is to reduce noise) is, according to Eq. (5.65), positive. That is to say, destabilizing feedback actually puts back into beam \hat{b}_3 some of the squeezing lost through the beam-splitter. Since the required round-loop gain (5.65) is less than unity, the feedback loop remains stable (see Section 5.2.3).

This result highlights the nonclassical nature of squeezed fluctuations. When an amplitude-squeezed beam strikes a beam-splitter, the intensity at one output port is anticorrelated with that at the other, hence the need for positive feedback. Of course, the feedback can never put more squeezing into the beam than was present at the start. That is, $S_3^X(\omega)_{\text{opt}}$ always lies between $S_0^X(\omega)$ and $S_3^X(\omega)|_{g=0}$. However, if we take the limit $\eta_1 \rightarrow 1$ and $S_0^X(\omega) \rightarrow 0$ (perfect squeezing to begin with) then all of this squeezing can be recovered, for any η_2 .

5.3 Feedback with optical beams using nonlinear optics

5.3.1 QND measurements

Section 5.2.2 showed that it was not possible to create squeezed light in the conventional sense using ordinary photodetection and linear feedback. Although the quantum theory appeared to show that the light which fell on the detector in the feedback loop was sub-shot noise, this could not be extracted because it was demolished by the detector. An obvious way around this would be to use a QND quadrature detector to control the feedback modulation. One way to achieve a QND measurement is for fields of different frequency to interact via a nonlinear refractive index. In order to obtain a large effect, large intensities are required. It is easiest to build up large intensities by using a resonant cavity. To describe this requires the quantum Langevin equations (QLEs) and input–output theory presented in Section 4.7.

Consider the apparatus shown in Fig. 5.2. The purpose of the detector in the feedback loop is to make a QND measurement of the quadrature X_{in}^b of the field $\hat{b}_{\text{in}} \equiv \hat{b}_1$. This field drives a cavity mode with decay rate κ described by annihilation operator \hat{a} . This mode is coupled to a second mode with annihilation operator \hat{c} and decay rate γ . We will assume an ideal QND coupling between the two modes

$$\hat{H} = \frac{\chi}{2} \hat{x}^a \hat{y}^c, \quad (5.68)$$

where

$$\hat{x}^a = \hat{a} + \hat{a}^\dagger; \quad \hat{y}^c = -i\hat{c} + i\hat{c}^\dagger. \quad (5.69)$$

As described in [AMW88], this Hamiltonian could in principle be realized by two simultaneous processes, assuming that modes a and c have the same frequency. The first process would be simple linear mixing of the modes (e.g. by an intracavity beam-splitter). The second process would require an intracavity crystal with a $\chi^{(2)}$ nonlinearity, pumped by a classical field at twice the frequency of modes a and c . The Hamiltonian (5.68) commutes with the x^a quadrature of mode a , and causes this to drive the x^c quadrature of mode c . Thus measuring the X_{out}^d quadrature of the output field \hat{d}_{out} from mode c will give a QND measurement of $\hat{a} + \hat{a}^\dagger$, which is approximately a QND measurement of \hat{X}_{in}^b .

The QLEs in the interaction frame for the quadrature operators are

$$\frac{d}{dt} \hat{x}^a = -\frac{\kappa}{2} \hat{x}^a - \sqrt{\kappa} \hat{X}_{\text{in}}^b, \quad (5.70)$$

$$\frac{d}{dt} \hat{x}^c = -\frac{\gamma}{2} \hat{x}^c - \sqrt{\gamma} \hat{X}_{\text{in}}^d + \chi \hat{x}^a. \quad (5.71)$$

Exercise 5.7 *Derive these.*

These can be solved in the frequency domain as

$$\tilde{X}^a(\omega) = -\frac{\sqrt{\kappa} \tilde{X}_{\text{in}}^b(\omega)}{\kappa/2 + i\omega}, \quad (5.72)$$

$$\tilde{X}^c(\omega) = -\frac{\sqrt{\gamma} \tilde{X}_{\text{in}}^d(\omega) + \sqrt{\kappa} \chi \tilde{X}_{\text{in}}^b(\omega)/(\kappa/2 + i\omega)}{\gamma/2 + i\omega}. \quad (5.73)$$

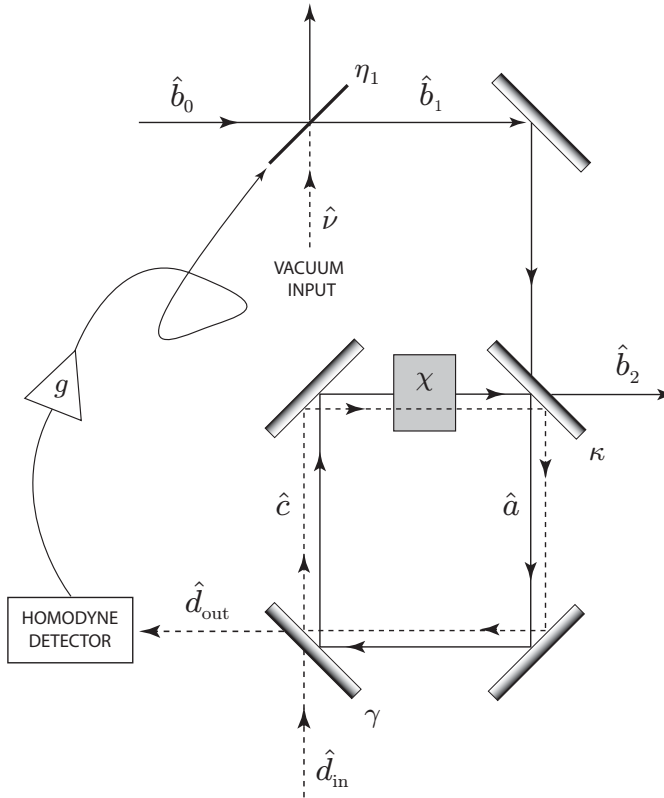


Fig. 5.2 A diagram for a travelling-wave feedback experiment based on a QND measurement. Travelling fields are denoted b and d . The first beam-splitter transmittance η_1 is variable. A cavity (drawn as a ring cavity for convenience) supports two modes, a (solid line) and c (dashed line). The decay rates for these two modes are κ and γ , respectively. They are coupled by a nonlinear optical process indicated by the crystal labelled χ . The perfect homodyne detection at the detector yields a photocurrent proportional to $\hat{X}_{\text{out}}^d = \hat{d}_{\text{out}} + \hat{d}_{\text{out}}^\dagger$. *Quantum Squeezing*, 2004, pp. 171–122, Chapter 6 ‘Squeezing and Feedback’, H. M. Wiseman, Figure 6.2, Springer-Verlag, Berlin, Heidelberg. Redrawn and revised and adapted with kind permission of Springer Science+Business Media.

The quadrature of the output field $\hat{d}_{\text{out}} = \hat{d}_{\text{in}} + \sqrt{\gamma}\hat{c}$ is therefore

$$\tilde{X}_{\text{out}}^d(\omega) = -\frac{\gamma\kappa Q \tilde{X}_{\text{in}}^b(\omega)/(\kappa + 2i\omega) + (\gamma - 2i\omega)\tilde{X}_{\text{in}}^d(\omega)}{\gamma + 2i\omega}, \quad (5.74)$$

where we have defined a quality factor for the measurement

$$Q = 4\chi/\sqrt{\gamma\kappa}. \quad (5.75)$$

In the limits $Q \gg 1$, and $\omega \ll \kappa, \gamma$, we have

$$\tilde{X}_{\text{out}}^d(\omega) \simeq -Q\tilde{X}_{\text{in}}^b(\omega), \quad (5.76)$$

which shows that a measurement (by homodyne detection) of the X quadrature of \hat{d}_{out} can indeed effect a measurement of the low-frequency variation in \hat{X}_{in}^b .

To see that this measurement is a QND measurement, we have to calculate the statistics of the output field from mode a , that is \hat{b}_{out} . From the solution (5.72) we find

$$\tilde{X}_{\text{out}}^b(\omega) = -\frac{\kappa/2 - i\omega}{\kappa/2 + i\omega} \tilde{X}_{\text{in}}^b(\omega). \quad (5.77)$$

That is, for frequencies small compared with κ , the output field is identical to the input field, as required for a QND measurement. Of course, we cannot expect the other quadrature to remain unaffected, because of the uncertainty principle. Indeed, we find

$$\tilde{Y}_{\text{out}}^b(\omega) = -\frac{\kappa - 2i\omega}{\kappa + 2i\omega} \tilde{Y}_{\text{in}}^b(\omega) + \frac{Q\gamma\kappa \tilde{Y}_{\text{in}}^d(\omega)/(\gamma + 2i\omega)}{\kappa + 2i\omega}, \quad (5.78)$$

which shows that noise has been added to \hat{Y}_{in} . Indeed, in the good measurement limit which gave the result (5.76), we find the phase quadrature output to be dominated by noise:

$$\tilde{Y}_{\text{out}}^b(\omega) \simeq Q\tilde{Y}_{\text{in}}^d(\omega). \quad (5.79)$$

5.3.2 QND-based feedback

We now wish to show how a QND measurement, such as that just considered, can be used to produce squeezing via feedback. The physical details of how the feedback can be achieved are as outlined in Section 5.2.2. In particular, in the limit that the transmittance η_1 of the modulated beam-splitter goes to unity, the effect of the modulation is simply to add an arbitrary signal to the amplitude quadrature of the controlled beam. That is, the modulated beam can be taken to be

$$\hat{b}_1(t) = \hat{b}_0(t - \tau_1) + \beta \frac{1}{2} \delta\eta_1(t - \tau_1), \quad (5.80)$$

where \hat{b}_0 is the beam incident on the modulated beam-splitter, as in Section 5.2.2. In the present case, $\hat{b}_1(t)$ is then fed into the QND device, as shown in Fig. 5.2, so $\hat{b}_{\text{in}}(t) = \hat{b}_1(t)$ again, and the modulation is controlled by the photocurrent from an (assumed perfect) homodyne measurement of X_{out}^d :

$$\delta\hat{\eta}_1(t) = \frac{g}{-Q\beta} \int_0^\infty h(t') \hat{X}_{\text{out}}^d(t - \tau_0 - t') dt'. \quad (5.81)$$

Here τ_0 is the delay time in the feedback loop, including the time of flight from the cavity for mode c to the homodyne detector, and $h(t)$ is as before.

On substituting Eqs. (5.80) and (5.81) into the results of the preceding subsection we find

$$\tilde{X}_{\text{out}}^b(\omega) = -\frac{\kappa - 2i\omega}{\kappa + 2i\omega} \frac{\tilde{X}_{\text{in}}^b(\omega) + \tilde{X}_{\text{in}}^d(\omega)g\tilde{h}(\omega)Q^{-1}(\gamma - 2i\omega)/(\gamma + 2i\omega)}{1 - g\tilde{p}(\omega)\tilde{h}(\omega)\exp(-i\omega T)}, \quad (5.82)$$

where $T = \tau_1 + \tau_0$ is the total round-trip delay time and

$$\tilde{p}(\omega) = \frac{\gamma\kappa}{(\kappa + 2i\omega)(\gamma + 2i\omega)} \quad (5.83)$$

represents the frequency response of the two cavity modes. If we assume that the field \hat{d}_{in} is in the vacuum state then we can evaluate the spectrum of amplitude fluctuations in \hat{X}_{out}^b to be

$$S_{\text{out}}^X(\omega) = \frac{S_{\text{in}}^X(\omega) + g^2 Q^{-2}}{|1 - g\tilde{p}(\omega)\tilde{h}(\omega)\exp(-i\omega T)|^2}. \quad (5.84)$$

Clearly, for a sufficiently high-quality measurement ($Q \rightarrow \infty$), the added noise term in the amplitude spectrum can be ignored. Then, for sufficiently large negative g , the feedback will produce a sub-shot-noise spectrum. Note the difference between this case and that of Section 5.2.2. Here the squeezed light is not part of the feedback loop; it is a free beam. The ultimate limit to how squeezed the beam can be is determined by the noise in the measurement, as will be discussed in Section 5.3.4.

Since \hat{b}_{out} is a free field, not part of any feedback loop, it should obey the standard commutation relations. This is the case, as can be verified from the expression (5.78) for \hat{Y}_{out}^b (which is unaffected by the feedback). Consequently, the spectrum for the phase quadrature

$$S_{\text{out}}^Y(\omega) = S_{\text{in}}^Y(\omega) + |Q\tilde{p}(\omega)|^2 \quad (5.85)$$

shows the expected increase in noise.

Exercise 5.8 Derive Eqs. (5.84) and (5.85) and verify that the uncertainty product $S_{\text{out}}^Y(\omega)S_{\text{out}}^X(\omega)$ is always greater than or equal to unity, as required for free fields.

5.3.3 Parametric down-conversion

The preceding section showed that feedback based on a perfect QND measurement can produce squeezing. This has never been done experimentally because of the difficulty of building a perfect QND measurement apparatus. However, it turns out that QND measurements are not the only way to produce squeezing via feedback. Any mechanism that produces correlations between the beam of interest and another beam that are more ‘quantum’ than the correlations between the two outputs of a linear beam-splitter can be the basis for producing squeezing via feedback. Such a mechanism must involve some sort of optical nonlinearity, hence the title of Section 5.3.

The production of amplitude squeezing by feeding back a quantum-correlated signal was predicted [JW85] and observed [WJ85b] by Walker and Jakeman in 1985, using the process of parametric down-conversion. An improved feedback scheme for the same system was later used by Tapster, Rarity and Satchell [TRS88] to obtain an inferred amplitude spectrum $S_1^X(\omega)_{\text{min}} = 0.72$ over a limited frequency range.

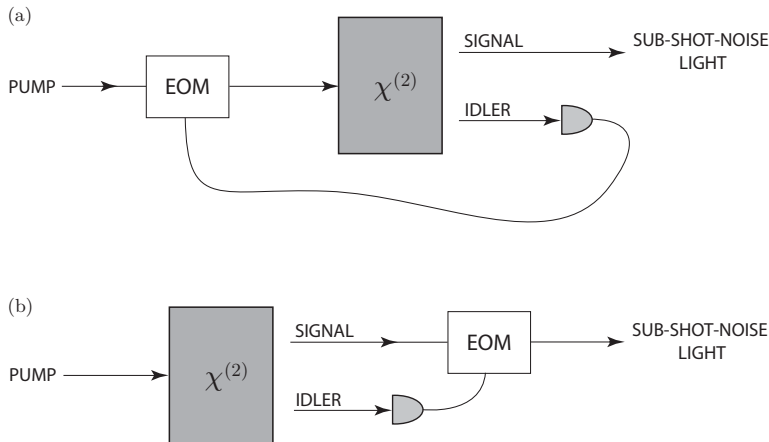


Fig. 5.3 A diagram showing two ways of producing sub-shot-noise light from parametric down-conversion. (a) Feedback, as first used by Walker and Jakeman [WJ85b]. (b) Feedforward, as first used by Mertz *et al.* [MHF⁺90]. Figure 1 adapted with permission from J. Mertz *et al.*, *Phys. Rev. A* **44**, 3229, (1991). Copyrighted by the American Physical Society.

The essential idea is as follows. Non-degenerate parametric down-conversion can be realized by pumping a crystal with a $\chi^{(2)}$ nonlinearity by a laser of frequency ω_1 and momentum \mathbf{k}_1 . For particular choices of ω_1 the crystal can be aligned so that a pump photon can be transformed into a pair of photons with frequencies ω_2, ω_3 and momenta $\mathbf{k}_2, \mathbf{k}_3$ with $\omega_1 = \omega_2 + \omega_3$ and $\mathbf{k}_1 = \mathbf{k}_2 + \mathbf{k}_3$. A special case (taking place inside a pair of cavities, for two modes with $\omega_2 = \omega_3$) has been mentioned already in Section 5.3.1. A pair of down-converted photons will thus be correlated in time because they are produced from a single pump photon. On a more macroscopic level, this means that the amplitude quadrature fluctuations in the two down-converted beams are positively correlated, and the correlation coefficient can in principle be very close to unity. In this ideal limit, measuring the intensity of beam 2 (called the idler) should give a readout identical to that obtained from measuring beam 3 (the signal). In effect, the measurement of the idler is like a QND measurement of the signal. Thus, feeding back the photocurrent from the idler with a negative gain should be able to reduce the noise in the signal below the shot-noise limit, as shown in Fig. 5.3(a).

5.3.4 Feedback, feedforward and robustness

In Refs. [WJ85b, TRS88] the negative feedback was effected by controlling the power of the pump laser (which controls the rate at which photon pairs are produced). This maintains the symmetry of the experiment so that the photocurrent fed back from the idler has the same statistics as the photocurrent from the free beam, the signal. In other words, they will both be below the shot noise, whereas without feedback they are both above the shot noise. However, it is not necessary to preserve the symmetry in this way. The measured

photocurrent from the idler can be fed *forwards* to control the amplitude fluctuations in the signal (for example by using an electro-optic modulator as described in Section 5.2.2). This feedforward was realized experimentally by Mertz *et al.* [MHF⁺90, MHF91], achieving similar results to that obtained by feedback. The two schemes are contrasted in Fig. 5.3.

Thus, unless one is concerned with light inside a feedback loop, there is no difference in theory between feedback and feedforward. Indeed, the squeezing produced by QND-based feedback discussed in Section 5.3.2 could equally well have been produced by QND-based feedforward. However, from a practical point of view, feedback has the advantage of being more *robust* with respect to parameter uncertainties.

Consider the QND-based feedback in Section 5.3.2, and for simplicity allow the QND cavity to be very heavily damped and the feedback to be very fast so that we may make the approximation $\tilde{h}(\omega)\exp(-i\omega T) = 1$. Also, say that the input light is coherent so that $S_{\text{in}}^X(\omega) = 1$. Then the output amplitude spectrum reduces to

$$S_{\text{out}}^X = \frac{1 + g^2 Q^{-2}}{(1 - g)^2}. \quad (5.86)$$

This has a minimum of

$$S_{\text{out};\text{min}}^X = (1 + Q^2)^{-1} \quad (5.87)$$

at $g = -Q^2$. For large Q (high-quality QND measurement) this is much less than unity.

Let us say that the experimenter does not know Q precisely, or cannot control g precisely, so that in the experiment the actual feedback loop has

$$g = -Q^2(1 + \epsilon), \quad (5.88)$$

where ϵ is a small relative error. To second order in ϵ this gives a new squeezed noise level of

$$S_{\text{out}}^X = (1 + Q^2)^{-1} \left[1 + \frac{\epsilon^2}{1 + Q^2} \right]. \quad (5.89)$$

Exercise 5.9 *Show this.*

The relative size of the extra noise term decreases with increasing Q , and, as long as $|\epsilon| \ll Q$, the increase in the noise level is negligible.

Now consider feedforward. Under the above conditions, the measured current is represented by the operator

$$\hat{X}_{\text{out}}^d = Q\hat{X}_{\text{in}}^b + \hat{X}_{\text{in}}^d. \quad (5.90)$$

This is fed forwards to create a coherent field of amplitude $(g/Q)\hat{X}_{\text{out}}^d$, which is added to the output of the system. Here g is the feedforward gain and the new output of the system will be

$$\hat{X}_{\text{out}}^b = \hat{X}_{\text{in}}^b + g(\hat{X}_{\text{in}}^b + \hat{X}_{\text{in}}^d/Q). \quad (5.91)$$

This has a noise level of

$$S_{\text{out}}^X = (1 + g)^2 + g^2 Q^{-2}, \quad (5.92)$$

which has a minimum of

$$S_{\text{out};\text{min}}^X = (1 + Q^2)^{-1}, \quad (5.93)$$

exactly the same as in the feedback case (as expected), but with an open-loop gain of $g = -Q^2/(1 + Q^2)$.

The difference between feedback and feedforward comes when we consider systematic errors. Again assuming a relative error in g of ϵ , so that

$$g = -\frac{Q^2(1 + \epsilon)}{1 + Q^2}, \quad (5.94)$$

the new noise level is exactly given by

$$S_{\text{out}}^X = (1 + Q^2)^{-1}(1 + Q^2\epsilon^2). \quad (5.95)$$

Now the relative size of the extra term actually *increases* as the quality of the measurement increases. In order for this term to be negligible, the systematic error must be extremely small: $|\epsilon| \ll Q^{-1}$. Thus, the feedforward approach is much less robust with respect to systematic errors due to uncertainties in the system parameters or inability to control the modulation exactly. This is a generic advantage of feedback over feedforward, and justifies our emphasis on the former in this book.

In the example above the distinction between feedback and feedforward is obvious. In the former case the measurement record (the current) used for control is affected by the controls applied at earlier times; in the latter it is not. This distinction will always apply for a continuous (in time) control protocol. However, discrete protocols may also be considered, and indeed one can consider the case of a single measurement result being used to control the system. In this case, one could argue that all control protocols are necessarily feedforward. However, the term feedback is often used in that case also, and we will follow that loose usage at times.

5.4 Feedback control of a monitored system

Having considered feedback on continuum fields, we now turn to a sort of feedback that would be more familiar in conception to a classical control engineer: the feedback control of a monitored system. We are concerned with quantum, rather than classical, systems, but many of the ideas from classical control theory carry over. For instance, it is often more convenient to describe the feedback using the conditioned state of the system (which classically would be a probability distribution as explained in Chapter 1). This is as opposed to describing the feedback using equations for the system operators (which classically would be equations for the system variables). Of course, the two methods are equally valid, and we will cover both in the remaining sections. However, the quantum trajectory (i.e. conditioned

states) method will be seen in this chapter to be more useful in a number of applications, and often to have more explanatory power. These advantages are further developed in the next chapter. Hence we begin our treatment of feedback control of a quantum system by reconsidering quantum trajectories. In this section we consider jumpy trajectories (as arise from direct detection in quantum optics).

5.4.1 General feedback

Consider for simplicity an open quantum system with a single decoherence channel described by the Markovian master equation

$$\dot{\rho} = -i[\hat{H}, \rho] + \mathcal{D}[\hat{c}]\rho. \quad (5.96)$$

As derived in Section 4.2, the simplest unravelling for this master equation is in terms of quantum jumps. In quantum optics, these correspond to δ -function spikes in the photocurrent $I(t)$ that are interpreted as the detection of a photon emitted by the system. We restate Eq. (4.40), the SME for the conditioned state $\rho_I(t)$:

$$d\rho_I(t) = \{dN(t)\mathcal{G}[\hat{c}] - dt\mathcal{H}[i\hat{H} + \frac{1}{2}\hat{c}^\dagger\hat{c}]\}\rho_I(t), \quad (5.97)$$

where the point process $dN(t) = I(t)dt$ is defined by

$$E[dN(t)] = \text{Tr}[\hat{c}^\dagger\hat{c}\rho_I(t)], \quad (5.98)$$

$$dN(t)^2 = dN(t). \quad (5.99)$$

The current $I(t) = dN/dt$ could be used to alter the system dynamics in many different ways. Some examples from quantum optics are the following: modulating the pump rate of a laser, the amplitude of a driving field, the cavity length, or the cavity loss rate. The last three examples could be effected by using an electro-optic modulator (a device with a refractive index controlled by a current), possibly in combination with a polarization-dependent beam-splitter. The most general expression for the effect of the feedback would be

$$[\dot{\rho}_I(t)]_{\text{fb}} = \mathcal{F}[t, \mathbf{I}_{[0,t)}]\rho_I(t). \quad (5.100)$$

Here $\mathbf{I}_{[0,t)}$ represents the complete photocurrent record from the beginning of the experiment up to the present time. Thus the superoperator $\mathcal{F}[t, \mathbf{I}_{[0,t)}]$ (which may be explicitly time-dependent) is a *functional* of the current for all past times. This functional dependence describes the response of the feedback loop, which may be nonlinear, and realistically must include some smoothing in time. The complete description of this feedback is given simply by adding Eq. (5.100) to Eq. (5.97). In general the resulting equation would have to be solved by numerical simulation.

To make progress towards understanding quantum feedback control, it is helpful to make simplifying assumptions. Firstly, let us consider a linear functional giving feedback

evolution of the form

$$[\dot{\rho}_I(t)]_{\text{fb}} = \int_0^\infty h(s)I(t-s)\mathcal{K}\rho_I(t)ds, \quad (5.101)$$

where \mathcal{K} is an arbitrary Liouville superoperator. Later in this section we will consider the Markovian limit in which the response function $h(s)$ goes to $\delta(s)$. To find this limit, it is first useful to consider the case $h(s) = \delta(s - \tau)$, where the feedback has a fixed delay τ . Then the feedback evolution is

$$[\dot{\rho}_I(t)]_{\text{fb}} = I(t - \tau)\mathcal{K}\rho_I(t). \quad (5.102)$$

Because there is no smoothing response function in Eq. (5.102), the right-hand side of the equation is a mathematically singular object, with $I(t)$ being a string of δ -functions. If it is meant to describe a physical feedback mechanism, then it is necessary to interpret the equation as an implicit stochastic differential equation, as explained in Section B.6. This is indicated already in the notation of using a fluxion on the left-hand side. The alternative interpretation as the explicit equation

$$[d\rho_I(t)]_{\text{fb}} = dN(t - \tau)\mathcal{K}\rho_I(t) \quad (5.103)$$

yields nonsense.

Exercise 5.10 Show that Eq. (5.103) does not even preserve positivity.

In order to combine Eq. (5.102) with Eq. (5.97), it is necessary to convert it from an implicit to an explicit equation. As explained in Section B.6, this is easy to accomplish because of the linearity (with respect to ρ) of Eq. (5.102). The result is

$$\rho_I(t) + [d\rho_I(t)]_{\text{fb}} = \exp[\mathcal{K}dN(t - \tau)]\rho_I(t). \quad (5.104)$$

Using the rule (5.99) and adding this evolution to that of the SME (5.97) gives the total conditioned evolution of the system

$$d\rho_I(t) = \{dN(t)\mathcal{G}[\hat{c}] - dt\mathcal{H}[\hat{H} + \frac{1}{2}\hat{c}^\dagger\hat{c}] + dN(t - \tau)(e^{\mathcal{K}} - 1)\}\rho_I(t). \quad (5.105)$$

It is not possible to turn this stochastic equation into a master equation by taking an ensemble average, as was possible with Eq. (5.97). This is because the feedback noise term (with argument $t - \tau$) is not independent of the state at time t . Physically, it is not possible to derive a master equation because the evolution including feedback (with a time delay) is not Markovian.

5.4.2 The feedback master equation

In order to make Eq. (5.105) more useful, it would be desirable to take the Markovian limit ($\tau \rightarrow 0$) in order to derive a non-selective master equation. Simply putting $\tau = 0$ in this equation and taking the ensemble average using Eq. (5.98) fails. The resultant evolution equation would be nonlinear in ρ and so could not be a valid master equation.

Exercise 5.11 *Show this.*

The reason why the nonlinearity is admissible in Eq. (5.105) is that ρ_I is a conditioned state for an individual system, not the unconditioned state $\rho = E[\rho_I]$. Physically, putting $\tau = 0$ fails because the feedback must act after the measurement even in the Markovian limit. The correct limit can be achieved by the equation

$$\rho_I(t + dt) = \exp[dN(t - \tau)\mathcal{K}]\{1 + dN(t)\mathcal{G}[\hat{c}] + dt \mathcal{H}[-i\hat{H} - \frac{1}{2}\hat{c}^\dagger\hat{c}]\}\rho_I(t). \quad (5.106)$$

For τ finite, this reproduces Eq. (5.105). However, if $\tau = 0$, expanding the exponential gives

$$d\rho_I(t) = \{dN(t)[e^{\mathcal{K}}(\mathcal{G}[\hat{c}] + 1) - 1] + dt \mathcal{H}[-i\hat{H} - \frac{1}{2}\hat{c}^\dagger\hat{c}]\}\rho_I(t). \quad (5.107)$$

In this equation, it is possible to take the ensemble average because $dN(t)$ can simply be replaced by its expectation value (5.98), giving

$$\dot{\rho} = e^{\mathcal{K}}\mathcal{J}[\hat{c}]\rho - \mathcal{A}[\hat{c}]\rho - i[\hat{H}, \rho] = \mathcal{L}\rho. \quad (5.108)$$

Recall from Eq. (1.80) that $\mathcal{J}[\hat{A}]\hat{b} \equiv \hat{A}\hat{b}\hat{A}^\dagger$, while

$$\mathcal{A}[\hat{A}]\hat{B} = \frac{1}{2}\{\hat{A}^\dagger\hat{A}\hat{B} + \hat{B}\hat{A}^\dagger\hat{A}\}. \quad (5.109)$$

Exercise 5.12 *Derive Eqs. (5.107) and (5.108), and show that the latter is of the Lindblad form.*

Hint: Remember that $e^{\mathcal{K}}$ is an operation.

That is, we have a new master equation incorporating the effect of the feedback. This master equation could have been guessed from an understanding of quantum jumps. However, the derivation here has the advantage of making clear the relation of the superoperator \mathcal{K} to experiment via Eq. (5.102). In the special case in which $\mathcal{K}\rho = -i[\hat{Z}, \rho]$, the conditioned SME with feedback can also be expressed as a SSE of the form of Eq. (4.19), with \hat{c} replaced by $e^{-i\hat{Z}}\hat{c}$.

Producing nonclassical light. Just as feedback based on absorptive photodetection cannot create a free squeezed beam (as shown in Section 5.2) by linear optics, so feedback based on direct detection cannot create a nonclassical state of a cavity mode by linear optics. By linear optics we mean processes that take coherent states to coherent states: linear damping, driving and detuning. By a nonclassical state we mean one that cannot be expressed as a mixture of coherent states. This concept of nonclassicality is really just a statement of what sort of quantum states are easy to produce, like the concept of the standard quantum limit.

In the present case, we can understand this limitation on feedback by considering the quantum trajectories. Both the jump and the no-jump evolution for a freely decaying cavity take a coherent state to a coherent state, in the former case with no change and in the latter with exponential decay of its amplitude.

Exercise 5.13 Show this.

Hint: First show that the measurement operators, for a decay rate γ , can be written as

$$\hat{M}_1(dt) = \sqrt{\gamma dt} \hat{a}, \quad \hat{M}_0(dt) = \exp(-\hat{a}^\dagger \hat{a} \gamma dt/2), \quad (5.110)$$

and recall Exercise 3.29.

If the post-jump feedback evolution $e^{\mathcal{K}}$ also takes a coherent state to a coherent state (or to a mixture of coherent states), it is clear that a nonclassical state can never be produced.

However, just as in the case of beams, feedback can cause the in-loop photocurrent to have nonclassical statistics. For direct detection the simplest form of nonclassical statistics is sub-Poissonian statistics. That is, the number of photons detected in some time interval has a variance less than its mean. For a field in a coherent state, the statistics will be Poissonian, and for a process that produces a mixture of coherent states (of different intensities) the statistics will be super-Poissonian.

In the quantum trajectory formalism, the explanation for anomalous (e.g. sub-Poissonian) in-loop photocurrent statistics lies in the modification of the jump measurement operator by the feedback as in Eq. (5.107). That is, the in-loop photocurrent autocorrelation function (from which the statistics can be determined) is modified from Eq. (4.50) to

$$E[I(t')I(t)] = \text{Tr}\left[\gamma \hat{a}^\dagger \hat{a} e^{\mathcal{L}(t'-t)} e^{\mathcal{K}} \gamma \hat{a} \rho(t) \hat{a}^\dagger\right] + \text{Tr}[\gamma \hat{a}^\dagger \hat{a} \rho(t)] \delta(t' - t), \quad (5.111)$$

where \mathcal{L} is as defined in Eq. (5.108) with $\hat{c} = \sqrt{\gamma} \hat{a}$.

Exercise 5.14 Show this using the same style of argument as in Section 4.3.2.

It is the effect of the feedback specific to the in-loop current via $e^{\mathcal{K}}$, not the overall evolution including feedback via $e^{\mathcal{L}(t'-t)}$, that may cause the sub-Poissonian in-loop statistics even if only linear optics is involved.

5.4.3 Application: protecting Schrödinger's cat

We now give an application (not yet experimentally realized) for Markovian feedback based on direct detection that shows the usefulness of the quantum trajectory approach. This example is due to Horoshko and Kilin [HK97].

In Section 3.9.1 we showed how damping of an oscillator leads to the rapid destruction of quantum coherence terms in a macroscopic superposition of two coherent states (a Schrödinger-cat state). Consider the particular cat state defined by

$$|\alpha; \phi\rangle_{\text{cat}} = [2(1 + e^{-2|\alpha|^2} \cos \phi)]^{-1/2} (|\alpha\rangle + e^{i\phi} |-\alpha\rangle). \quad (5.112)$$

Under the damping master equation

$$\dot{\rho} = \gamma \mathcal{D}[\hat{a}] \rho, \quad (5.113)$$

the quantum coherence terms in ρ decay as $\exp(-2\gamma|\alpha|^2 t)$, while the coherent amplitudes themselves decay as $\exp(-\gamma t/2)$ (see Section 3.9.1).

If we consider a direct-detection unravelling of this master equation, then the no-jump evolution leads solely to the decay of the coherent amplitudes.

Exercise 5.15 *Show this.*

Thus it is the jumps that are responsible for the destruction of the superposition. This makes sense, since the rate of decay of the coherence terms scales as the rate of jumps. We can see explicitly how this happens from the following:

$$\hat{a}|\alpha; \phi\rangle_{\text{cat}} \propto \alpha[|\alpha\rangle - e^{i\phi}|- \alpha\rangle] \propto |\alpha; \phi - \pi\rangle_{\text{cat}}. \quad (5.114)$$

That is, upon a detection the phase of the superposition changes by π , which leads to the decoherence.

Exercise 5.16 *Show that, for $|\alpha| \gg 1$, an equal mixture of $|\alpha; \phi\rangle_{\text{cat}}$ and $|\alpha; \phi - \pi\rangle_{\text{cat}}$ has no coherence, since it is the same as an equal mixture of $|\alpha\rangle$ and $|- \alpha\rangle$.*

Of course, if one keeps track of the detections then one knows which cat state the system is in at all times. (A similar analysis of the case for homodyne detection is done in Ref. [CKT94].) It would be preferable, however, to have a deterministic cat state. If one had arbitrary control over the cavity state then this could always be done by feedback following each detection since any two pure states are always unitarily related. However, this observation is not particularly interesting unless the feedback can be implemented with a practically realizable interaction. As Horoshko and Kilin pointed out, for the state $|\alpha; \pi/2\rangle_{\text{cat}}$ this is the case, since a simple rotation of the state in phase-space has the following effect:

$$e^{-i\pi\hat{a}^\dagger\hat{a}}|\alpha; -\pi/2\rangle_{\text{cat}} = -i|\alpha; \pi/2\rangle_{\text{cat}}. \quad (5.115)$$

That is, if one uses the feedback Hamiltonian

$$\hat{H}_{\text{fb}}(t) = I(t)\pi\hat{a}^\dagger\hat{a}, \quad (5.116)$$

with $I(t)$ the photocurrent from direct detection of the cavity output, then, following each detection that causes ϕ to change from $\pi/2$ to $-\pi/2$, the feedback changes ϕ back to $\pi/2$. Thus the effect of the jumps is nullified, and the time-evolved state is simply $|\alpha e^{-\gamma t/2}; \pi/2\rangle_{\text{cat}}$.

Exercise 5.17 *Verify Eq. (5.115) and also that $|\alpha e^{-\gamma t/2}; \pi/2\rangle_{\text{cat}}$ is a solution of the feedback-modified master equation*

$$\dot{\rho} = \gamma \mathcal{D}[e^{-i\pi\hat{a}^\dagger\hat{a}}\hat{a}]\rho.$$

Practicalities of optical feedback. Physically, the Hamiltonian (5.116) requires the ability to control the frequency of the cavity mode. Provided that it is done slowly enough, this can be achieved simply by changing the physical properties of the cavity, such as its length, or

the refractive index of some material inside it. Here ‘slowly enough’ means slow compared with the separation of the eigenstates of the Hamiltonian, so that the adiabatic theorem [BF28] applies. Assuming we can treat just a single mode in the cavity (as will be the case if it is small enough), this energy separation equals the resonance frequency ω_0 . On the other hand, the δ -function in Eq. (5.116) implies a modulation that is fast enough for one to ignore any other evolution during its application. As we have seen, the fastest of the two evolution rates in the problem (without feedback) is $2\gamma|\alpha|^2$. Thus the time-scale T for the modulation of the cavity frequency must satisfy

$$\gamma|\alpha|^2 \ll T^{-1} \ll \omega_0. \quad (5.117)$$

Now $\gamma \ll \omega_0$ is necessary for the derivation of the master equation (5.113). Moreover, a typical ratio on these time-scales (the quality factor of the cavity) is of order 10^8 . Thus, if both \ll signs in Eq. (5.117) are assumed to be satisfied by ratios of 10^{-2} , the scheme could protect Schrödinger cats with $|\alpha| \sim 100$, which is arguably macroscopic. In practice, other physical limitations are going to be even more important.

First, realistic feedback will not be Markovian, but will have some time delay τ . For the Markovian approximation to be valid, this must be much less than the time-scale for photon loss: $\tau^{-1} \gg \gamma|\alpha|^2$. Even with very fast detectors and electronics it would be difficult to make the effective delay τ less than 10 ns [SRO⁺02]. Also, even very good optical cavities have γ at least of order 10^4 s^{-1} . Again assuming that the above inequality is satisfied by a factor of 10^2 , the limit now becomes $|\alpha| \sim 10$.

Second, realistic detectors do not have unit efficiency, as discussed in Section 4.8.1. For photon counting, as required here, $\eta = 0.9$ is an exceptionally good figure at present. Taking into account inefficiency, the feedback-modified master equation is

$$\dot{\rho} = \gamma\eta\mathcal{D}[e^{-i\pi\hat{a}^\dagger\hat{a}}\hat{a}]\rho + \gamma(1-\eta)\mathcal{D}[\hat{a}]\rho. \quad (5.118)$$

Even with $\eta = 0.9$ the decay rate for the coherence terms, $2\gamma(1-\eta)|\alpha|^2$, will still be greater than the decay rate for the coherent amplitude, $\gamma/2$, unless $|\alpha| \sim 1.5$ or smaller. In other words, until ultra-high-efficiency photodetectors are manufactured, it is only Schrödinger ‘kittens’ that may be protected to any significant degree.

5.4.4 Feedback in the Heisenberg picture

The example in the preceding subsection shows how useful the quantum trajectory analysis is for designing feedback control of a quantum system, and how convenient the Schrödinger picture (in particular the feedback-modified master equation) is for determining the effect of the feedback. Nevertheless, it is possible to treat feedback control of a quantum system in the Heisenberg picture, as we used for the propagating fields in Sections 5.1 and 5.2. In this section, we present that theory.

Recall from Eq. (4.35) that the unitary operator generating the system and bath evolution for an infinitesimal interval is

$$\hat{U}_0(t + dt, t) = \exp[\hat{c} d\hat{B}_0(t)^\dagger - \hat{c}^\dagger d\hat{B}_0(t) - i\hat{H} dt]. \quad (5.119)$$

Here $d\hat{B}_0 = \hat{b}_0(t)dt$, where \hat{b}_0 is the annihilation operator for the input field which is in the vacuum state, so that $d\hat{B}_0 d\hat{B}_0^\dagger = dt$ but all other second-order moments vanish. Using this, we obtain the QLE for an arbitrary system operator corresponding to the master equation (5.96):

$$d\hat{s} = \hat{U}_0^\dagger(t + dt, t)\hat{s}\hat{U}_0(t + dt, t) - \hat{s} \quad (5.120)$$

$$= i[\hat{H}, \hat{s}]dt + (\hat{c}^\dagger \hat{s} \hat{c} - \frac{1}{2} \hat{s} \hat{c}^\dagger \hat{c} - \frac{1}{2} \hat{c}^\dagger \hat{c} \hat{s})dt - [d\hat{B}_0^\dagger \hat{c} - \hat{c}^\dagger d\hat{B}_0, \hat{s}]. \quad (5.121)$$

Similarly, the output field is the infinitesimally evolved input field:

$$\begin{aligned} \hat{b}_1(t) &= \hat{U}_0^\dagger(t + dt, t)\hat{b}_0(t)\hat{U}_0(t + dt, t) \\ &= \hat{b}_0(t) + \hat{c}(t). \end{aligned} \quad (5.122)$$

The output photon-flux operator (equivalent to the photocurrent derived from a perfect detection of that field) is $\hat{I}_1(t) = \hat{b}_1^\dagger(t)\hat{b}_1(t)$. This suggests that the feedback considered in Section 5.4.1 could be treated in the Heisenberg picture by using the feedback Hamiltonian

$$\hat{H}_{fb}(t) = \hat{I}_1(t - \tau)\hat{Z}(t), \quad (5.123)$$

where each of these quantities is an operator. Here, the feedback superoperator \mathcal{K} used in Section 5.4.1 would be defined by $\mathcal{K}\rho = -i[\hat{Z}, \rho]$. The generalization to arbitrary \mathcal{K} would be possible by involving auxiliary systems.

It might be thought that there is an ambiguity of operator ordering in Eq. (5.123), because \hat{I}_1 contains system operators. In fact, the ordering is not important because $\hat{b}_1(t)$ commutes with all system operators at a later time as discussed in Section 4.7.1, so $\hat{I}_1(t)$ does also. Of course, $\hat{b}_1(t)$ will not commute with system operators for times after $t + \tau$ (when the feedback acts), but $\hat{I}_1(t)$ still will because it is not changed by the feedback interaction. (It commutes with the feedback Hamiltonian.) This fact would allow one to use the formalism developed here to treat feedback of a photocurrent smoothed by time-averaging. That is to say, there is still no operator-ordering ambiguity in the expression

$$\hat{H}_{fb}(t) = \hat{Z}(t) \int_0^\infty h(s)\hat{I}_1(t - s)ds, \quad (5.124)$$

or even for a general Hamiltonian functional of the current, as in Eq. (5.100). For a sufficiently broad response function $h(s)$, there is no need to use stochastic calculus for the feedback; the explicit equation of motion due to the feedback would simply be

$$d\hat{s}(t) = i[\hat{H}_{fb}(t), \hat{s}(t)]dt. \quad (5.125)$$

However, this approach makes the Markovian limit difficult to find. Thus, as in Section 5.4.1, the response function will be assumed to consist of a time delay only, as in Eq. (5.123).

In order to treat Eq. (5.123) it is necessary once again to use the stochastic calculus of Appendix B to find the explicit effect of the feedback. As in Section 3.11.1, the key is to expand the unitary operator for feedback

$$\hat{U}_{\text{fb}}(t + dt, t) = \exp[-i\hat{H}_{\text{fb}}(t)dt] \quad (5.126)$$

to as many orders as necessary. Since this evolution commutes with the no-feedback evolution (5.121), the feedback simply adds the following extra term to Eq. (5.121):

$$[d\hat{s}]_{\text{fb}} = \hat{U}_{\text{fb}}^\dagger(t + dt, t)\hat{s}(t)\hat{U}_{\text{fb}}(t + dt, t) - \hat{s}(t), \quad (5.127)$$

which evaluates to

$$[d\hat{s}]_{\text{fb}} = d\hat{N}_1(t - \tau)\left(e^{i\hat{Z}}\hat{s}e^{-i\hat{Z}} - \hat{s}\right). \quad (5.128)$$

Exercise 5.18 *Show this.*

Including the no-feedback evolution and expanding $d\hat{N}_1(t)$ using Eq. (5.122) gives

$$\begin{aligned} d\hat{s} = & i[\hat{H}, \hat{s}]dt + \left(\hat{c}^\dagger\hat{s}\hat{c} - \frac{1}{2}\hat{s}\hat{c}^\dagger\hat{c} - \frac{1}{2}\hat{c}^\dagger\hat{c}\hat{s}\right)dt - [d\hat{B}_0^\dagger\hat{c} - \hat{c}^\dagger d\hat{B}_0, \hat{s}] \\ & + [\hat{c}^\dagger(t - \tau) + \hat{b}_0^\dagger(t - \tau)]\left(e^{i\hat{Z}}\hat{s}e^{-i\hat{Z}} - \hat{s}\right)[\hat{c}(t - \tau) + \hat{b}_0(t - \tau)]dt. \end{aligned} \quad (5.129)$$

Exercise 5.19 *Verify that this is a valid non-Markovian QLE. That is to say, that, for arbitrary system operators \hat{s}_1 and \hat{s}_2 , $d(\hat{s}_1\hat{s}_2)$ is correctly given by $(d\hat{s}_1)\hat{s}_2 + \hat{s}_1(d\hat{s}_2) + (d\hat{s}_1)(d\hat{s}_2)$.*

Again, all time arguments are t unless otherwise indicated. This should be compared with Eq. (5.105). The obvious difference is that Eq. (5.105) explicitly describes direct photodetection, followed by feedback, whereas the irreversibility in Eq. (5.129) does not specify that the output has been detected. Indeed, the original Langevin equation (5.121) is unchanged if the output is subject to homodyne detection, rather than direct detection. This is the essential difference between the quantum fluctuations of Eq. (5.129) and the fluctuations due to information gathering in Eq. (5.105).

5.4.5 Markovian feedback in the Heisenberg picture

In Eq. (5.129), the vacuum field operators $\hat{b}_0(t)$ have deliberately been moved to the outside (using the fact that $\hat{b}_1(t - \tau)$ commutes with system operators at time t). This has been done for convenience, because, in this position, they disappear when the trace is taken over the bath density operator. Taking the total trace over system and bath density operators gives

$$\begin{aligned} \langle d\hat{s} \rangle = & \langle i[\hat{H}, \hat{s}] + \left(\hat{c}^\dagger\hat{s}\hat{c} - \frac{1}{2}\hat{s}\hat{c}^\dagger\hat{c} - \frac{1}{2}\hat{c}^\dagger\hat{c}\hat{s}\right)dt \\ & + \left\langle \hat{c}^\dagger(t - \tau)\left(e^{i\hat{Z}}\hat{s}e^{-i\hat{Z}} - \hat{s}\right)\hat{c}(t - \tau) \right\rangle dt. \end{aligned} \quad (5.130)$$

In the limit $\tau \rightarrow 0$, so that $\hat{c}(t - \tau)$ differs negligibly from $\hat{c}(t)$, this gives

$$\langle d\hat{s} \rangle = \left\langle i[\hat{H}, \hat{s}] + (\hat{c}^\dagger \hat{s} \hat{c} - \frac{1}{2} \hat{s} \hat{c}^\dagger \hat{c} - \frac{1}{2} \hat{c}^\dagger \hat{c} \hat{s}) + \hat{c}^\dagger (e^{i\hat{Z}} \hat{s} e^{-i\hat{Z}} - \hat{s}) \hat{c} \right\rangle dt. \quad (5.131)$$

In terms of the system density operator,

$$\langle d\hat{s} \rangle = \text{Tr} \left[\hat{s} \left(-i[\hat{H}, \rho] + \mathcal{D}[e^{-i\hat{Z}} \hat{c}] \rho \right) dt \right]. \quad (5.132)$$

This is precisely what would have been obtained from the Markovian feedback master equation (5.108) for $\mathcal{K}\rho = -i[\hat{Z}, \rho]$.

Moreover, it is possible to set $\tau = 0$ in Eq. (5.129) and still obtain a valid QLE:

$$\begin{aligned} d\hat{s} = & i[\hat{H}, \hat{s}]dt - [\hat{s}, \hat{c}^\dagger] \left(\frac{1}{2} \hat{c} + \hat{b}_0 \right) dt + \left(\frac{1}{2} \hat{c}^\dagger + \hat{b}_0^\dagger \right) [\hat{s}, \hat{c}] dt \\ & + (\hat{c}^\dagger + \hat{b}_0^\dagger) \left(e^{i\hat{Z}} \hat{s} e^{-i\hat{Z}} - \hat{s} \right) (\hat{c} + \hat{b}_0) dt. \end{aligned} \quad (5.133)$$

This equation is quite different from Eq. (5.129) because it is Markovian. This implies that, in this equation, it is no longer possible freely to move $\hat{b}_1 = (\hat{c} + \hat{b}_0)$, since it now has the same time argument as the other operators, rather than an earlier one.

Exercise 5.20 Show that Eq. (5.133) is a valid QLE, bearing in mind that now it is \hat{b}_0 rather than \hat{b}_1 that commutes with all system operators.

This trick with time arguments and commutation relations enables the correct QLE describing feedback to be derived without worrying about the method of dealing with the $\tau \rightarrow 0$ limit used in Section 5.4.2. There are subtleties involved in using this method in the Heisenberg picture, as will become apparent in Section 5.5.3.

5.5 Homodyne-mediated feedback control

Although homodyne detection can be considered the limit of a jump process (see Section 4.4), it is convenient to develop separately the theory of quantum feedback of currents with Gaussian white noise. In fact, it is necessary to do so in order to treat feedback based on homodyne detection in the presence of a broad-band non-vacuum bath, as we will do.

5.5.1 The homodyne feedback master equation

As shown in Section 4.8.1, the SME for homodyne detection of efficiency η is

$$d\rho_J(t) = -i[\hat{H}, \rho_J(t)]dt + dt \mathcal{D}[\hat{c}]\rho_J(t) + \sqrt{\eta} dW(t) \mathcal{H}[\hat{c}]\rho_J(t). \quad (5.134)$$

The homodyne photocurrent, normalized so that the deterministic part does not depend on the efficiency, is

$$J_{\text{hom}}(t) = \langle \hat{x} \rangle_J(t) + \xi(t)/\sqrt{\eta}, \quad (5.135)$$

where $\xi(t) = dW(t)/dt$ and $\hat{x} = \hat{c} + \hat{c}^\dagger$ as usual. Unlike the direct-detection photocurrent, this current may be negative because the constant local oscillator background has been subtracted. This means that, if one were to feed back this current as in Section 5.4.1, with

$$[\dot{\rho}_J(t)]_{\text{fb}} = J_{\text{hom}}(t - \tau) \mathcal{K} \rho_J(t), \quad (5.136)$$

then the superoperator \mathcal{K} must be such as to give valid evolution irrespective of the sign of time. That is to say, it must give reversible evolution with

$$\mathcal{K} \rho \equiv -i[\hat{F}, \rho] \quad (5.137)$$

for some Hermitian operator \hat{F} .

To treat this feedback we use a similar analysis to that of Section 5.4. The only difference is that, because the stochasticity in the measurement (5.134) and the feedback (5.136) is Gaussian white noise, the feedback superoperator $\exp[\mathcal{K} J_{\text{hom}}(t - \tau) dt]$ need only be expanded to second order. The result for the total conditioned evolution of the system is

$$\begin{aligned} \rho_J(t + dt) = & \left\{ 1 + \mathcal{K}[\langle \hat{c} + \hat{c}^\dagger \rangle_J(t - \tau) dt + dW(t - \tau)/\sqrt{\eta}] + [1/(2\eta)] \mathcal{K}^2 dt \right\} \\ & \times \left\{ 1 + \mathcal{H}[-i\hat{H}] dt + \mathcal{D}[\hat{c}] dt + \sqrt{\eta} dW(t) \mathcal{H}[\hat{c}] \right\} \rho_J(t). \end{aligned} \quad (5.138)$$

For τ finite, this becomes

$$\begin{aligned} d\rho_J(t) = dt & \left\{ \mathcal{H}[-i\hat{H}] + \mathcal{D}[\hat{c}] + \langle \hat{c} + \hat{c}^\dagger \rangle_J(t - \tau) \mathcal{K} + \frac{1}{2\eta} \mathcal{K}^2 \right\} \rho_J(t) \\ & + dW(t - \tau) \mathcal{K} \rho_J(t) / \sqrt{\eta} + \sqrt{\eta} dW(t) \mathcal{H}[\hat{c}] \rho_J(t). \end{aligned} \quad (5.139)$$

On the other hand, putting $\tau = 0$ in Eq. (5.138) gives

$$\begin{aligned} d\rho_J(t) = dt & \left\{ -i[\hat{H}, \rho_J(t)] + \mathcal{D}[\hat{c}] \rho_J(t) - i[\hat{F}, \hat{c} \rho_J(t) + \rho_J(t) \hat{c}^\dagger] \right\} \\ & + dt \mathcal{D}[\hat{F}] \rho_J(t) / \eta + dW(t) \mathcal{H}[\sqrt{\eta} \hat{c} - i\hat{F} / \sqrt{\eta}] \rho_J(t). \end{aligned} \quad (5.140)$$

For $\eta = 1$ and an initially pure state, this can be alternatively be expressed as a SSE. Ignoring normalization, this is simply

$$d|\bar{\psi}_J(t)\rangle = dt \left[-i\hat{H} - \frac{1}{2}(\hat{c}^\dagger \hat{c} + 2i\hat{F}\hat{c} + \hat{F}^2) + J_{\text{hom}}(t)(\hat{c} - i\hat{F}) \right] |\bar{\psi}_J(t)\rangle. \quad (5.141)$$

Exercise 5.21 Verify this, by finding the SME for $\bar{\rho}_J \equiv |\bar{\psi}_J\rangle\langle\bar{\psi}_J|$ and then adding the terms necessary to preserve the norm.

The non-selective evolution of the system is easier to find from the SME (5.140). This is a true Itô equation, so that taking the ensemble average simply removes the stochastic term. This gives the homodyne feedback master equation

$$\dot{\rho} = -i[\hat{H}, \rho] + \mathcal{D}[\hat{c}] \rho - i[\hat{F}, \hat{c} \rho + \rho \hat{c}^\dagger] + \frac{1}{\eta} \mathcal{D}[\hat{F}] \rho. \quad (5.142)$$

An equation of this form was derived by Caves and Milburn [CM87] for an idealized model for position measurement plus feedback, with \hat{c} replaced by \hat{x} and η set to 1. The first feedback term, linear in \hat{F} , is the desired effect of the feedback which would dominate in the classical regime. The second feedback term causes diffusion in the variable conjugate to \hat{F} . It can be attributed to the inevitable introduction of noise by the measurement step in the quantum-limited feedback loop. The lower the efficiency, the more noise introduced.

The homodyne feedback master equation can be rewritten in the Lindblad form (4.28) as

$$\dot{\rho} = -i[\hat{H} + \frac{1}{2}(\hat{c}^\dagger \hat{F} + \hat{F} \hat{c}), \rho] + \mathcal{D}[\hat{c} - i\hat{F}]\rho + \frac{1-\eta}{\eta} \mathcal{D}[\hat{F}]\rho \equiv \mathcal{L}\rho. \quad (5.143)$$

In this arrangement, the effect of the feedback is seen to replace \hat{c} by $\hat{c} - i\hat{F}$ and to add an extra term to the Hamiltonian, plus an extra diffusion term that vanishes for perfect detection. In what follows, η will be assumed to be unity unless stated otherwise, since the generalization is usually obvious from previous examples.

The two-time correlation function of the current can be found from Eq. (5.140) to be

$$E[J_{\text{hom}}(t')J_{\text{hom}}(t)] = \text{Tr}\left\{(\hat{c} + \hat{c}^\dagger)e^{\mathcal{L}(t'-t)}[(\hat{c} - i\hat{F})\rho(t) + \text{H.c.}]\right\} + \delta(\tau). \quad (5.144)$$

Exercise 5.22 Verify this using the method of Section 4.4.4.

Again, note that the feedback affects the term in square brackets, as well as the evolution by \mathcal{L} for time $t' - t$. This means that the in-loop photocurrent may have a sub-shot-noise spectrum, even if the light in the cavity dynamics is classical. From the same reasoning as in Section 5.4.2, the feedback will not produce nonclassical dynamics for a damped harmonic oscillator ($\hat{c} \propto \hat{a}$) if \hat{F} is a Hamiltonian corresponding to linear optical processes, that is, if \hat{F} is linear in \hat{a} or proportional to $\hat{a}^\dagger \hat{a}$.

5.5.2 Feedback with white noise

From one point of view, the results just obtained are simply a special case of those of Section 5.4. Consider the quantum jump SME for homodyne detection with finite local oscillator amplitude, as in Eq. (4.66). Now add feedback according to

$$[\dot{\rho}_J(t)]_{\text{fb}} = -i[\hat{F}, \rho_J(t)] \frac{dN(t) - \gamma^2 dt}{\gamma dt}, \quad (5.145)$$

where this is understood to be the $\tau \rightarrow 0$ limit. Using Section 5.4, the feedback master equation is

$$\dot{\rho} = -i[\hat{H} + i\frac{1}{2}(-\hat{c}\gamma + \hat{c}^\dagger\gamma) - \hat{F}\gamma, \rho] + \mathcal{D}[e^{-i\hat{F}/\gamma}(\hat{c} + \gamma)]\rho. \quad (5.146)$$

Expanding the exponential to second order in $1/\gamma$ and then taking the limit $\gamma \rightarrow \infty$ reproduces (5.143). The correlation functions follow similarly as a special case.

Exercise 5.23 Show these results.

However, in another sense, feedback based on homodyne detection is more general: it is possible to treat detection, and hence feedback, in the presence of thermal or squeezed white noise, as in Section 4.8.2.

The relevant conditioning equation for homodyne detection with a white-noise bath parameterized by N and M is Eq. (4.253), reproduced here:

$$d\rho_J(t) = \left\{ dt \mathcal{L} + \frac{1}{\sqrt{L}} dW(t) \mathcal{H}[(N + M^* + 1)\hat{c} - (N + M)\hat{c}^\dagger] \right\} \rho_c(t), \quad (5.147)$$

where $L = 2N + M + M^* + 1$, and the photocurrent is

$$J_{\text{hom}}(t) = \langle \hat{c} + \hat{c}^\dagger \rangle_J(t) + \sqrt{L} \xi(t). \quad (5.148)$$

Adding feedback as in Eq. (5.136), which is the same as introducing a feedback Hamiltonian

$$\hat{H}_{\text{fb}}(t) = \hat{F} J_{\text{hom}}(t), \quad (5.149)$$

and following the method above yields the master equation

$$\begin{aligned} \dot{\rho} = & (N + 1) \{ \mathcal{D}[\hat{c}] \rho - i[\hat{F}, \hat{c} \rho + \rho \hat{c}^\dagger] \} + N \{ \mathcal{D}[\hat{c}^\dagger] \rho + i[\hat{F}, \hat{c}^\dagger \rho + \rho \hat{c}] \} \\ & + M \{ \tfrac{1}{2} [\hat{c}^\dagger, [\hat{c}^\dagger, \rho]] + i[\hat{F}, [\hat{c}^\dagger, \rho]] \} + M^* \{ \tfrac{1}{2} [\hat{c}, [\hat{c}, \rho]] - i[\hat{F}, [\hat{c}, \rho]] \} \\ & + L \mathcal{D}[\hat{F}] \rho - i[\hat{H}, \rho]. \end{aligned} \quad (5.150)$$

For the case $N = M = 0$, this reduces to Eq. (5.142) with $\eta = 1$.

5.5.3 Homodyne feedback in the Heisenberg picture

The quantum Langevin treatment of quadrature flux feedback (corresponding to homodyne detection) is relatively straightforward, because of the Gaussian nature of the noise. The homodyne photocurrent is identified with the quadrature of the outgoing field,

$$\hat{J}_{\text{hom}}(t) = \hat{b}_1(t) + \hat{b}_1^\dagger(t) = \hat{c}(t) + \hat{c}^\dagger(t) + \hat{b}_0(t) + \hat{b}_0^\dagger(t). \quad (5.151)$$

The feedback Hamiltonian is defined as

$$\hat{H}_{\text{fb}}(t) = \hat{F}(t) \hat{J}_{\text{hom}}(t - \tau). \quad (5.152)$$

The time delay τ ensures that the output quadrature operator $\hat{J}_{\text{hom}}(t - \tau)$ commutes with all system operators at time t . Thus, it will commute with $\hat{F}(t)$ and there is no ambiguity in the operator ordering in Eq. (5.152). Treating the equation of motion generated by this Hamiltonian as a Stratonovich (or implicit) equation, the Itô (or explicit) equation is

$$[d\hat{s}(t)]_{\text{fb}} = i \hat{J}_{\text{hom}}(t - \tau) [\hat{F}(t), \hat{s}(t)] dt - \tfrac{1}{2} [\hat{F}(t), [\hat{F}(t), \hat{s}(t)]] dt. \quad (5.153)$$

Adding in the non-feedback evolution gives the total explicit equation of motion

$$\begin{aligned} d\hat{s} = & i[\hat{H}, \hat{s}]dt + i[\hat{c}^\dagger(t - \tau)dt + d\hat{B}_0^\dagger(t - \tau)][\hat{F}, \hat{s}] \\ & + i[\hat{F}, \hat{s}][\hat{c}(t - \tau)dt + d\hat{B}_0(t - \tau)] - \frac{1}{2}[\hat{F}, [\hat{F}, \hat{s}]]dt \\ & + (\hat{c}^\dagger\hat{s}\hat{c} - \frac{1}{2}\hat{s}\hat{c}^\dagger\hat{c} - \frac{1}{2}\hat{c}^\dagger\hat{c}\hat{s})dt - [d\hat{B}_0^\dagger\hat{c} - \hat{c}^\dagger d\hat{B}_0, \hat{s}]. \end{aligned} \quad (5.154)$$

Here, all time arguments are t unless indicated otherwise.

In Eq. (5.154), we have once again used the commutability of the output operators with system operators to place them suitably on the exterior of the feedback expression. This ensures that, when an expectation value is taken, the input noise operators annihilate the vacuum and hence give no contribution. This is the same trick as used in Section 5.4.4, and putting $\tau = 0$ in Eq. (5.154) also gives a valid Heisenberg equation of motion. That equation is the counterpart to the homodyne feedback master equation (5.143). However, this trick will not work if the input field is not in the vacuum state, but rather, for example, in a thermal state. For direct detection (without filtering), it is necessary to restrict to a vacuum bath, in which case the operator-ordering trick is perfectly legitimate. However, for quadrature-based feedback, as explained in Section 5.5.2, it is possible to treat white noise. Thus, it is necessary to have a method of treating the Markovian ($\tau \rightarrow 0$) limit that will work in this general case (although we will not present the general theory here). The necessary method is essentially the same as that used with the quantum trajectories, ensuring that the feedback acts later than the measurement. In applying it to Heisenberg equations of motion, it will be seen that one has to be quite careful with operator ordering.

In the $\tau = 0$ limit the feedback Hamiltonian (5.152) has an ordering ambiguity, because the bath operator $\hat{b}_1(t)$ does not commute with an arbitrary system operator $\hat{s}(t)$ at the same time. This problem would not occur if the feedback Hamiltonian were instead

$$\hat{H}_0^{\text{fb}}(t) = \hat{F}(t)[\hat{b}_0(t) + \hat{b}_0^\dagger(t)], \quad (5.155)$$

because $\hat{b}_0(t)$ does commute with $\hat{s}(t)$. At first sight it would not seem sensible to use Eq. (5.155) because $\hat{b}_0(t) + \hat{b}_0^\dagger(t)$ is the quadrature of the vacuum input, which is independent of the system and so (it would seem) cannot describe feedback. However, Eq. (5.155) is the correct Hamiltonian to use as long as we ensure that the feedback-coupling between the system and the bath occurs *after* the usual coupling between system and bath. That is, the total unitary operator evolving the system and bath at time t is

$$\hat{U}(t + dt, t) = e^{-i\hat{H}_0^{\text{fb}}(t)dt} \hat{U}_0(t + dt, t), \quad (5.156)$$

where $\hat{U}_0(t + dt, t)$ is defined in Eq. (5.119). In the Heisenberg picture, the system evolves via

$$\hat{s}(t + dt) = \hat{U}^\dagger(t + dt, t)\hat{s}(t)\hat{U}(t + dt, t) \quad (5.157)$$

$$= \hat{U}_0^\dagger(t + dt, t)e^{+i\hat{H}_0^{\text{fb}}(t)dt}\hat{s}(t)e^{-i\hat{H}_0^{\text{fb}}(t)dt}\hat{U}_0(t + dt, t). \quad (5.158)$$

Note that in Eq. (5.158) the feedback appears to act first because of the reversal of the order of unitary operators in the Heisenberg picture. If desired, one could rewrite Eq. (5.158) in a (perhaps) more intuitive order as

$$\hat{s}(t + dt) = e^{+i\hat{H}_1^{\text{fb}}(t)dt} \hat{U}_0^\dagger(t + dt, t) \hat{s}(t) \hat{U}_0(t + dt, t) e^{-i\hat{H}_1^{\text{fb}}(t)dt}. \quad (5.159)$$

Here

$$\hat{H}_1^{\text{fb}}(t) = \hat{U}_0^\dagger(t + dt, t) \hat{H}_0^{\text{fb}}(t) \hat{U}_0(t + dt, t) \quad (5.160)$$

$$= \hat{F}(t + dt) \hat{J}_{\text{hom}}(t). \quad (5.161)$$

That is, we regain the output quadrature (or homodyne photocurrent operator), as well as replacing $\hat{F}(t)$ by $\hat{F}(t + dt)$. This ensures that, once again, there is no operator ambiguity in Eq. (5.161) because the \hat{J}_{hom} represents the result of the homodyne measurement at a time t earlier (albeit infinitesimally) than the time argument for the system operator \hat{F} . Again, this makes sense physically because the feedback must act after the measurement.

Expanding the exponentials in Eq. (5.158) or Eq. (5.159), the quantum Itô rules give

$$\begin{aligned} d\hat{s} = & i[\hat{H}, \hat{s}]dt - [\hat{s}, \hat{c}^\dagger] \left(\frac{1}{2} \hat{c} dt + d\hat{B}_0 \right) + \left(\frac{1}{2} \hat{c}^\dagger dt + d\hat{B}_0^\dagger \right) [\hat{s}, \hat{c}] \\ & + i[\hat{c}^\dagger dt + d\hat{B}_0^\dagger][\hat{F}, \hat{s}] + i[\hat{F}, \hat{s}][\hat{c} dt + d\hat{B}_0] - \frac{1}{2}[\hat{F}, [\hat{F}, \hat{s}]]dt. \end{aligned} \quad (5.162)$$

Exercise 5.24 Verify this, and show that this is a valid Markovian QLE that is equivalent to the homodyne feedback master equation (5.142).

5.6 Markovian feedback in a linear system

In order to understand the nature of quantum-limited feedback, it is useful to consider a simple linear system that can be solved exactly. We use the example of Ref. [WM94c]: a single optical mode in a cavity, so that the two quadratures x and y , obeying $[\hat{x}, \hat{y}] = 2i$, form a complete set of observables. To obtain linear equations of motion for these observables it is necessary first to restrict the Hamiltonian \hat{H} to be a quadratic function of \hat{x} and \hat{y} . Second, the Lindblad operator \hat{c} must be a linear function of \hat{x} and \hat{y} , which it will be for cavity damping in which $\hat{c} = \hat{a} = (\hat{x} + i\hat{y})/2$. Third, the measured current must be a linear function of these variables, as in homodyne detection of the cavity output (which is what we will assume). Finally, the feedback Hamiltonian must be such that \hat{F} is a linear function also, as in classical driving of a cavity. These basic ideas will be treated much more generally in Chapter 6.

5.6.1 The linear system

Since in this chapter we are seeking merely a simple example, we make the further assumption that we are interested only in \hat{x} and that it obeys a linear QLE independent of \hat{y} . In this case, all Markovian linear dynamics (in the absence of feedback) can be composed of

damping, driving and parametric driving. Damping will be assumed to be always present, since we will assume homodyne detection of the output field from our system. We therefore take the damping rate to be unity. Constant linear driving simply shifts the stationary state away from $\langle \hat{x} \rangle = 0$, and will be ignored. Stochastic linear driving in the white-noise approximation causes diffusion in the x quadrature, at a rate l . Finally, if the strength of the parametric driving ($\hat{H} \propto \hat{x}\hat{y} + \hat{y}\hat{x}$) is χ (where $\chi = 1$ would represent a parametric oscillator at threshold), then the master equation for the system is

$$\dot{\rho} = \mathcal{D}[\hat{a}]\rho + \frac{1}{4}l\mathcal{D}[\hat{a}^\dagger - \hat{a}]\rho + \frac{1}{4}\chi[\hat{a}^2 - \hat{a}^{\dagger 2}, \rho] \equiv \mathcal{L}_0\rho, \quad (5.163)$$

where \hat{a} is the annihilation operator for the cavity mode as above.

Although parametric driving is an example of a nonlinear optical process (which can generate nonclassical optical states such as squeezed states), it gives linear dynamics in that the mean and variance of $\hat{x} = \hat{a} + \hat{a}^\dagger$ obey linear equations of the following form:

$$\frac{d}{dt}\langle \hat{x} \rangle = -k\langle \hat{x} \rangle, \quad (5.164)$$

$$\frac{d}{dt}V = -2kV + D. \quad (5.165)$$

Exercise 5.25 Show that for the particular master equation above (the properties of which will be denoted by the subscript 0) these equations hold, with

$$k_0 = \frac{1}{2}(1 + \chi), \quad (5.166)$$

$$D_0 = 1 + l. \quad (5.167)$$

Hint: Remember that $d\langle \hat{x} \rangle/dt = \text{Tr}[\hat{x}\dot{\rho}]$ and that $d\langle \hat{x}^2 \rangle/dt = \text{Tr}[\hat{x}^2\dot{\rho}]$.

For a *stable* system with $k > 0$, there is a steady state with $\langle x \rangle = 0$ and

$$V = \frac{D}{2k}. \quad (5.168)$$

It turns out that the first two moments (the mean and variance) are actually sufficient to specify the stationary state of the system because it is a Gaussian state. That is, its Wigner function (see Section A.5) is Gaussian. The probability distribution for x (which is all we are interested in here) is just the marginal distribution for the Wigner function, so it is also Gaussian. Moreover, if the distribution is originally Gaussian (as for the vacuum, for example), then it will be Gaussian at all times. This can be seen by considering the equation of motion for the probability distribution for x ,

$$\wp(x) = \langle x | \rho | x \rangle. \quad (5.169)$$

This equation of motion can be derived from the master equation by considering the operator correspondences for the Wigner function (see Section A.5). Because here we have $[\hat{x}, \hat{y}] = 2i$, if we identify \hat{x} with \hat{Q} then we must identify \hat{y} with $2\hat{P}$. On doing this we find that

$\wp(x)$ obeys the following Fokker–Planck equation (see Section B.5)

$$\dot{\wp}(x) = \left(\frac{\partial}{\partial x} kx + \frac{1}{2} D \frac{\partial^2}{\partial x^2} \right) \wp(x). \quad (5.170)$$

This particular form, with linear drift kx and constant diffusion $D > 0$, is known as an Ornstein–Uhlenbeck equation (OUE).

Exercise 5.26 *Derive Eq. (5.170) from Eq. (5.163), and show by substitution that it has a Gaussian solution with mean and variance satisfying Eqs. (5.164) and (5.165), respectively.*

In the present case, $V_0 = (1 + l)/(1 + \chi)$. If this is less than unity, the system exhibits squeezing of the x quadrature. It is useful to characterize the squeezing by the normally ordered variance (see Section A.5)

$$U \equiv \langle \hat{a}^\dagger \hat{a}^\dagger + 2\hat{a}^\dagger \hat{a} + \hat{a} \hat{a} \rangle - \langle \hat{a}^\dagger + \hat{a} \rangle^2, \quad (5.171)$$

Exercise 5.27 *Show from this definition that $U = V - 1$.*

For this system, the normally ordered variance takes the value

$$U_0 = \frac{l - \chi}{1 + \chi}. \quad (5.172)$$

Now, if the system is to stay below threshold (so that the variance in the y quadrature does not become unbounded), then the maximum value for χ is unity.

Exercise 5.28 *Show this from the master equation (5.163)*

At this value, $U_0 = -1/2$ when the x -diffusion rate $l = 0$. Therefore the minimum value of squeezing which this linear system can attain as a stationary value is half of the theoretical minimum of $U_0 = -1$.

In quantum optics, the output light is often of more interest than the intracavity light. Therefore it is useful to compute the output noise statistics. For squeezed systems, the relevant quantity is the spectrum of the homodyne photocurrent, as introduced in Section 4.4.4,

$$S(\omega) = \lim_{t \rightarrow \infty} \int_{-\infty}^{\infty} d\tau \, \text{E}[J_{\text{hom}}(t + \tau) J_{\text{hom}}(t)] e^{-i\omega\tau}. \quad (5.173)$$

Given the drift and diffusion coefficients for the dynamics, the spectrum in the present case is

$$S(\omega) = 1 + \frac{D - 2k}{\omega^2 + k^2}. \quad (5.174)$$

Exercise 5.29 *Show this using the results from Section 4.4.4.*

Hint: Remember that, for example, $\text{Tr}[\hat{x} e^{\mathcal{L}\tau} (\hat{a} \rho_{\text{ss}})]$ is just the expectation value of \hat{x} at time τ using the ‘state’ with initial condition $\rho(0) = \hat{a} \rho_{\text{ss}}$. Thus, since the mean of \hat{x} obeys the linear equation (5.164), it follows that this expression simplifies to $e^{-k\tau} \text{Tr}[\hat{x} \hat{a} \rho_{\text{ss}}]$.

The spectrum consists of a constant term representing shot noise plus a Lorentzian, which will be negative for squeezed systems. The spectrum can be related to the intracavity squeezing by subtracting the vacuum noise:

$$\frac{1}{2\pi} \int_{-\infty}^{\infty} d\omega [S(\omega) - 1] = \frac{D - 2k}{2k} = U. \quad (5.175)$$

That is, the total squeezing integrated across all frequencies in the output is equal to the intracavity squeezing. However, the minimum squeezing, which for a simple linear system such as this will occur at zero frequency,² may be greater than or less than U . It is useful to define it by another parameter,

$$R = S(0) - 1 = 2U/k. \quad (5.176)$$

For the particular system considered above,

$$R_0 = \frac{l - \chi}{\frac{1}{4}(1 + \chi)^2}. \quad (5.177)$$

In the ideal limit ($\chi \rightarrow 1, l \rightarrow 0$), the zero-frequency squeezing approaches the minimum value of -1 .

5.6.2 Adding linear feedback

Now consider adding feedback to try to reduce the fluctuations in x . Restricting the feedback to linear optical processes suggests the feedback operator

$$\hat{F} = -\lambda \hat{y}/2. \quad (5.178)$$

As a separate Hamiltonian, this translates a state in the negative x direction for λ positive. By controlling this Hamiltonian by the homodyne photocurrent, one thus has the ability to change the statistics for x and perhaps achieve better squeezing. Substituting Eq. (5.178) into the general homodyne feedback master equation (5.142) and adding the free dynamics (5.163) gives

$$\dot{\rho} = \mathcal{L}_0 \rho + \frac{\lambda}{2} [\hat{a} - \hat{a}^\dagger, \hat{a} \rho + \rho \hat{a}^\dagger] + \frac{\lambda^2}{4\eta} \mathcal{D}[\hat{a} - \hat{a}^\dagger] \rho. \quad (5.179)$$

Here η is the proportion of output light used in the feedback loop, multiplied by the efficiency of the detection. For the x distribution $\wp(x)$ one finds that it still obeys an OUE, but now with

$$k = k_0 + \lambda, \quad (5.180)$$

$$D = D_0 + 2\lambda + \lambda^2/\eta. \quad (5.181)$$

² In reality, the minimum noise is never found at zero frequency, because virtually all experiments are subject to non-white noise of technical origin, which can usually be made negligible at high frequencies, but whose spectrum grows without bound as $\omega \rightarrow 0$. Often, the spectrum scales at $1/\omega$, or $1/f$, where $f = \omega/(2\pi)$, in which case it is known as $1/f$ noise.

Exercise 5.30 *Show this.*

Provided that $\lambda + k_0 > 0$, there will exist a stable Gaussian solution to the master equation (5.179). The new intracavity squeezing parameter is

$$U_\lambda = (k_0 + \lambda)^{-1} \left(k_0 U_0 + \frac{\lambda^2}{2\eta} \right). \quad (5.182)$$

An immediate consequence of this expression is that U_λ can be negative only if U_0 is. That is to say, the feedback cannot produce squeezing, as explained in Section 5.5. On minimizing U_λ with respect to λ one finds

$$U_{\min} = \eta^{-1} \left(-k_0 + \sqrt{k_0^2 + 2\eta k_0 U_0} \right), \quad (5.183)$$

when

$$\lambda = -k_0 + \sqrt{k_0^2 + 2\eta k_0 U_0}. \quad (5.184)$$

Note that this λ has the same sign as U_0 . That is to say, if the system produces squeezed light, then the best way to enhance the squeezing is to add a force that displaces the state in the direction of the difference between the measured photocurrent and the desired mean photocurrent. This positive feedback is the opposite of what would be expected classically, and can be attributed to the effect of homodyne measurement on squeezed states, as will be explained in Section 5.6.3. Obviously, the best intracavity squeezing will be when $\eta = 1$, in which case the intracavity squeezing can be simply expressed as

$$U_{\min} = k_0 \left(-1 + \sqrt{1 + R_0} \right). \quad (5.185)$$

Although linear optical feedback cannot produce squeezing, this does not mean that it cannot reduce noise. In fact, it can be proven that $U_{\min} \leq U_0$, with equality only if $\eta = 0$ or $U_0 = 0$.

Exercise 5.31 *Show this for $\eta = 1$ using the result $\sqrt{1 + R_0} \leq 1 + R_0/2$ (since $R_0 \geq -1$). The result for any η follows by application of the mean-value theorem.*

This result implies that the intracavity variance in x can always be reduced by homodyne-mediated linear optical feedback, unless it is at the vacuum noise level. In particular, intracavity squeezing can always be enhanced. For the parametric oscillator defined originally in Eq. (5.163), with $l = 0$, $U_{\min} = -\chi/\eta$. For $\eta = 1$, the (symmetrically ordered) x variance is $V_{\min} = 1 - \chi$. The y variance, which is unaffected by feedback, is seen from Eq. (5.163) to be $(1 - \chi)^{-1}$. Thus, with perfect detection, it is possible to produce a minimum-uncertainty squeezed state with arbitrarily high squeezing as $\chi \rightarrow 1$. This is not unexpected, since parametric driving in an undamped cavity also produces minimum-uncertainty squeezed states (but there is no steady state). The feedback removes the noise that was added by the damping that enables the measurement used in the feedback.

Next, we turn to the calculation of the output squeezing. Here, it must be remembered that at least a fraction η of the output light is being used in the feedback loop. Thus, the

fraction θ of cavity emission available as an output of the system is at best $1 - \eta$. Integrated over all frequencies, the total available output squeezing is thus θU_λ . It can be shown that

$$\theta U_{\min} \geq U_0 \text{ for } U_0 < 0. \quad (5.186)$$

Exercise 5.32 *Convince yourself that this is true.*

That is, dividing the cavity output and using some in a feedback loop produces worse squeezing in the remaining output than was present in the original, undivided output. Note, however, that, if the cavity output is inherently divided (which is often the case, with two output mirrors), then using one output in the feedback loop would enhance squeezing in the other output. This is because the squeezing in the system output of interest would have changed from θU_0 to θU_{\min} .

Rather than integrating over all frequencies, experimentalists are often more interested in the optimal noise reduction at some frequency, which is to say at zero frequency here. With no feedback, this is given by R_0 . With feedback, it is given by

$$R_\lambda = \theta \frac{2U_\lambda}{k_0 + \lambda} = \theta \frac{2k_0 U_0 + \lambda^2/\eta}{(k_0 + \lambda)^2}. \quad (5.187)$$

In all cases, R_λ is minimized for a different value of λ from that which minimizes U_λ . One finds

$$R_{\min} = \frac{\theta R_0}{1 + R_0 \eta} \quad (5.188)$$

when

$$\lambda = 2\eta U_0. \quad (5.189)$$

Again, λ has the same sign as U_0 . It follows immediately from Eq. (5.188) that, since $R_0 \geq -1$ and $\theta \leq 1 - \eta$,

$$R_{\min} \geq R_0 \text{ for } R_0 < 0. \quad (5.190)$$

That is to say, dividing the cavity output to add a homodyne-mediated classical feedback loop cannot produce better output squeezing at any frequency than would be available from an undivided output with no feedback. These ‘no-go’ results are analogous to those obtained for the feedback control of optical beams derived in Section 5.2.

5.6.3 Understanding feedback through conditioning

The preceding section gave the limits to noise reduction by classical feedback for a linear system, both intracavity and extracavity. In this section, we give an explanation for the intracavity results, in terms of the conditioning of the state by the measurement on which the feedback is based. To find this link between conditioning and feedback it is necessary to return to the selective stochastic master equation (5.138) for the conditioned state

matrix $\rho_J(t)$,

$$\begin{aligned} d\rho_J(t) = dt & \left(\mathcal{L}_0 \rho_J(t) + \mathcal{K}[a\rho_J(t) + \rho_J(t)a^\dagger] + \frac{1}{2\eta} \mathcal{K}^2 \rho_J(t) \right) \\ & + dW(t) (\sqrt{\eta} \mathcal{H}[\hat{a}] + \mathcal{K}/\sqrt{\eta}) \rho_J(t). \end{aligned} \quad (5.191)$$

Here, \mathcal{L}_0 is as defined in Eq. (5.163) and $\mathcal{K}\rho = -i[\hat{F}, \rho]$, where \hat{F} is defined in Eq. (5.178). Changing this to a stochastic FPE for the conditioned marginal Wigner function gives

$$\begin{aligned} d\wp_J(x) = dt & \left[\frac{\partial}{\partial x} (k_0 + \lambda)x + \frac{1}{2} \frac{\partial^2}{\partial x^2} (D_0 + 2\lambda + \lambda^2/\eta) \right] \wp_J(x) \\ & + dW(t) \left[\sqrt{\eta} \left(x - \bar{x}_J(t) + \frac{\partial}{\partial x} \right) + (\lambda/\sqrt{\eta}) \frac{\partial}{\partial x} \right] \wp_J(x), \end{aligned} \quad (5.192)$$

where $\bar{x}_J(t)$ is the mean of the distribution $\wp_J(x)$.

Exercise 5.33 Show this using the Wigner-function operator correspondences.

This equation is obviously no longer a simple OUE. Nevertheless, it still has a Gaussian as an exact solution. Specifically, the mean \bar{x}_J and variance V_J of the conditioned distribution obey the following equations (recall that $\xi(t) = dW/dt$):

$$\dot{\bar{x}}_J = -(k_0 + \lambda)\bar{x}_J + \xi(t) [\sqrt{\eta}(V_J - 1) - (\lambda/\sqrt{\eta})], \quad (5.193)$$

$$\dot{V}_J = -2k_0 V_J + D_0 - \eta(V_J - 1)^2. \quad (5.194)$$

Exercise 5.34 Show this by considering a Gaussian ansatz for Eq. (5.192).

Hint: Remember that, for any b , $1 + dW(t)b = \exp[dW(t)b - dt b^2/2]$.

Two points about the evolution equation for V_J are worth noting: it is completely deterministic (no noise terms); and it is not influenced by the presence of feedback.

The equation for the conditioned variance is more simply written in terms of the conditioned normally ordered variance $U_J = V_J - 1$,

$$\dot{U}_J = -2k_0 U_J - 2k_0 + D_0 - \eta U_J^2. \quad (5.195)$$

On a time-scale as short as a cavity lifetime, U_J will approach its steady-state value of

$$U_J^{\text{ss}} = \eta^{-1} \left(-k_0 + \sqrt{k_0^2 + \eta(-2k_0 + D_0)} \right). \quad (5.196)$$

Note that this is equal to the minimum *unconditioned* variance with feedback – the U_{\min} of Eq. (5.183). The explanation for this will become evident shortly. Substituting the steady-state conditioned variance into Eq. (5.193) gives

$$\dot{\bar{x}}_J = -(k_0 + \lambda)\bar{x}_J + \xi(t) \frac{1}{\sqrt{\eta}} \left[-k_0 + \sqrt{k_0^2 + \eta(-2k_0 + D_0)} - \lambda \right]. \quad (5.197)$$

If one were to choose $\lambda = -k_0 + \sqrt{k_0^2 + \eta(-2k_0 + D_0)}$ then there would be no noise at all in the conditioned mean and so one could set $\bar{x}_J = 0$ in steady state. This value of

λ is precisely that value derived as Eq. (5.184) to minimize the unconditioned variance under feedback. Now one can see why this minimum unconditioned variance is equal to the conditioned variance. The feedback works simply by suppressing the fluctuations in the conditioned mean.

In general, the unconditioned variance will consist of two terms, the conditioned quantum variance in x plus the classical (ensemble) average variance in the conditioned mean of x :

$$U_\lambda = U_J + E[\bar{x}_J^2]. \quad (5.198)$$

The latter term is found from Eq. (5.197) to be

$$E[\bar{x}_J^2] = \eta^{-1} \frac{1}{2(k_0 + \lambda)} \left[-(k_0 + \lambda) + \sqrt{k_0^2 + \eta(-2k_0 + D_0)} \right]^2. \quad (5.199)$$

Adding Eq. (5.196) gives

$$U_\lambda = \eta^{-1} \frac{1}{2(k_0 + \lambda)} [\lambda^2 + \eta(-2k_0 + D_0)]. \quad (5.200)$$

Exercise 5.35 *Verify that this is identical to the expression (5.182) derived in the preceding subsection using the unconditioned master equation.*

Using the conditioned equation, there is an obvious way to understand the feedback. The homodyne measurement reduces the conditioned variance (except when it is equal to the classical minimum of 1). The more efficient the measurement, the greater the reduction. Ordinarily, this reduced variance is not evident because the measurement gives a random shift to the conditional mean of x , with the randomness arising from the shot noise of the photocurrent. By appropriately feeding back this photocurrent, it is possible to counteract precisely this shift and thus observe the conditioned variance.

The sign of the feedback parameter λ is determined by the sign of the shift which the measurement gives to the conditioned mean \bar{x}_J . For classical statistics ($U \geq 0$), a higher than average photocurrent reading ($\xi(t) > 0$) leads to an increase in \bar{x}_J (except if $U = 0$, in which case the measurement has no effect). However, for nonclassical states with $U < 0$, the classical intuition fails since a positive photocurrent fluctuation causes \bar{x}_J to decrease. This explains the counter-intuitive negative value of λ required in squeezed systems, which naively would be thought to destabilize the system and increase fluctuations. However, the value of the positive feedback required, given by Eq. (5.184), is such that the overall decay rate $k_0 + \lambda$ is still positive.

It is worth remarking that the above conclusions are not limited to Markovian feedback, which is all that we have analysed. One could consider a feedback Hamiltonian proportional to an arbitrary (even nonlinear) function of the photocurrent $J(t)$, and the equation for the conditional variance (5.194) will remain exactly as it is. Only the equation for the mean will be changed. Although this equation might not be solvable, Eq. (5.198) guarantees that the unconditioned variance cannot be less than the conditional variance. Moreover, if the feedback Hamiltonian is a linear functional of the photocurrent then the equation for the mean will be solvable in Fourier space, provided that the feedback is stable. That is, for

linear systems one can solve for arbitrary feedback using the theory of quantum trajectories in exactly the same manner as we did for QLEs in Section 5.2. The interested reader is referred to Ref. [WM94c].

To conclude, one can state succinctly that conditioning can be made practical by feedback. The intracavity noise reduction produced by ‘classical’ feedback can never be better than that produced (conditionally) by the measurement. Of course, nonclassical feedback (such as using the photocurrent to influence nonlinear intracavity elements) may produce nonclassical states, but such elements can produce nonclassical states without feedback, so this is hardly surprising. In order to produce nonclassical states by feedback with linear optics, it would be necessary to have a nonclassical measurement scheme. That is to say, one that does not rely on measurement of the extracavity light to procure information about the intracavity state. For example, a QND measurement of one quadrature would produce a squeezed conditioned state and hence allow the production of unconditional intracavity (and extracavity) squeezing by feedback. Again, the interested reader is referred to Ref. [WM94c]. This is essentially the same conclusion as that which was reached for feedback on optical beams in Section 5.3. In the following section we consider feedback based on QND measurements in an atomic (rather than optical) system.

5.7 Deterministic spin-squeezing

Performing a QND measurement of an optical quadrature, as discussed in the preceding section and Section 5.3.1, is very difficult experimentally. However, for atomic systems it should be easier to achieve a QND measurement near the quantum limit. In this section we apply the theory developed in this chapter to the deterministic production of spin-squeezing, as proposed in Ref. [TMW02b]. Here the spin refers to the z component of angular momentum of atoms. A spin-squeezed state [KU93] is an entangled state of an ensemble of such atoms, such that the total z component of angular momentum has a smaller uncertainty than if all atoms were prepared identically without entanglement.

5.7.1 Spin-squeezing

Consider an atom with two relevant levels, with the population difference operator being the Pauli operator $\hat{\sigma}_z$. The collective properties of N such atoms prepared identically are conveniently described by a spin- J system for $J = N/2$. The collective angular-momentum operators, $\hat{\mathbf{J}}$, are $\hat{J}_\alpha = \sum_{k=1}^N \hat{j}_\alpha^{(k)}$, where $\alpha = x, y, z$ and where $\hat{j}_\alpha^{(k)} = \hat{\sigma}_\alpha^{(k)}/2$ is the angular-momentum operator for the k th atom. $\hat{\mathbf{J}}$ obey the cyclic commutation relations $[\hat{J}_x, \hat{J}_y] = i\epsilon_{xyz}\hat{J}_z$.

Exercise 5.36 *Verify this from the commutation relations for the Pauli matrices. See Box. 3.1.*

The corresponding uncertainty relations are

$$(\Delta J_y)^2(\Delta J_z)^2 \geq \frac{1}{4}|\langle J_x \rangle|^2, \quad (5.201)$$

plus cyclic permutations. The operator \hat{J}_z represents half the total population difference and is a quantity that can be measured, for example by dispersive imaging techniques as will be discussed.

For a coherent spin state (CSS) of a spin- J system, the elementary spins all point in the same direction, with no correlations. An example of such a state is a \hat{J}_x eigenstate of maximum eigenvalue $J = N/2$. Such a state achieves the minimum of the uncertainty relation (5.201), with the variance of the two components normal to the mean direction (in this case, J_z and J_y) equal to $J/2$. If quantum-mechanical correlations are introduced among the atoms it is possible to reduce the fluctuations in one direction at the expense of the other. This is the idea of a squeezed spin state (SSS) introduced by Kitagawa and Ueda [KU93]. That is, the spin system is squeezed when the variance of one spin component normal to the mean spin vector is smaller than the standard quantum limit (SQL) of $J/2$.

There are many ways to characterize the degree of spin-squeezing in a spin- J system. We will use the criteria of Sørensen and co-workers [SDCZ01] and Wang [Wan01], where the squeezing parameter is given by

$$\xi_{n_1}^2 = \frac{N(\Delta J_{n_1})^2}{\langle J_{n_2} \rangle^2 + \langle J_{n_3} \rangle^2}, \quad (5.202)$$

where $\hat{J}_n \equiv \mathbf{n} \cdot \hat{\mathbf{J}}$ and \mathbf{n}_i for $i = 1, 2, 3$ are orthogonal unit vectors. Systems with $\xi_n^2 < 1$ are said to be spin-squeezed in the direction \mathbf{n} . It has also been shown that this indicates that the atoms are in an entangled state [SDCZ01]. This parameter also has the appealing property that, for a CSS, $\xi_n^2 = 1$ for all n [Wan01]. In all that follows, we consider spin-squeezing in the z direction and hence drop the subscript on ξ^2 .

The ultimate limit to ξ^2 (set by the Heisenberg uncertainty relations) is of order $1/N$. Since N is typically very large experimentally (of order 10^{11}), the potential for noise reduction is enormous. However, so far, the degree of noise reduction achieved experimentally has been modest, with $\xi^2 \sim 10^{-1} \gg N^{-1}$. The amount of entanglement in such states is relatively small, so it is a good approximation to assume that the atoms are unentangled when evaluating the denominator of Eq. (5.202). That is, for example, if the mean spin is in the x direction, we can say that $\langle J_x \rangle = J$ and that $\langle J_y \rangle = \langle J_z \rangle = 0$. For squeezing in the z direction, the squeezing parameter is thus given by

$$\xi^2 \simeq \langle J_z^2 \rangle / (J/2). \quad (5.203)$$

Spin-squeezed states have potential applications in fields such as quantum information [JKP01] and high-precision time-keeping [WBI⁺92].

5.7.2 Measurement and feedback

Let the two relevant internal states of each atom be the magnetic sublevels of a $j = \frac{1}{2}$ state, such as the ground state of an alkali atom. In the absence of a magnetic field, these levels are degenerate. For such an atom, a probe beam that is suitably polarized and suitably detuned from a particular excited atomic level will not be absorbed by the atoms. Rather, it will suffer a phase shift of different size depending upon which state the atom is in. That is, the phase shift will be linear in the atomic operator \hat{J}_z . If all atoms are coupled equally to the probe beam then the total phase shift will depend only on the total spin operator \hat{J}_z . The phase shift can then be measured by homodyne detection.

A simple model for this that captures the most important physics of the measurement is the SME

$$d\rho_Y = MD[\hat{J}_z]\rho_Y dt + \sqrt{M} dW(t)\mathcal{H}[\hat{J}_z]\rho_Y. \quad (5.204)$$

Here ρ_Y is the state of the spin system conditioned on the current

$$Y(t) = 2\sqrt{M}\langle J_z \rangle_Y + dW(t)/dt, \quad (5.205)$$

where unit detection efficiency has been assumed. We are using $Y(t)$, rather than $J(t)$ as has been our convention, in order to avoid confusion with the total spin J . For a probe beam in free space, the QND measurement strength (with dimensions of T^{-1}) is

$$M = P\hbar\omega[\gamma^2/(8A\Delta I_{\text{sat}})]^2, \quad (5.206)$$

where P is the probe power, $\omega = 2\pi c/\lambda$ is the probe frequency, A is the cross-sectional area of the probe, γ is the spontaneous emission rate from the excited state and I_{sat} is the saturation intensity for the transition, which equals $2\pi^2\hbar\omega\gamma/\lambda^2$ for a two-level atom [Ash70]. Note that Eq. (5.204) ignores spontaneous emission by the atoms – for a discussion see Ref. [TMW02a] and for more complete treatments see Refs. [BSSM07, NM08].

Using optical pumping, the atomic sample can be prepared such that all the atoms are in one of their internal states. A fast $\pi/2$ -pulse can then be applied, coherently transferring all atoms into an equal superposition of the two internal states, which is an eigenstate of the \hat{J}_x operator with eigenvalue J . As described earlier, the CSS is a minimum-uncertainty state, so in this case the variances of both J_z and J_y are $J/2$.

The dominant effects of the conditioned evolution (5.204) on the initial CSS are a decrease in the uncertainty of J_z (since we are measuring J_z) with corresponding noise increases in J_y and J_x , and a stochastic shift of the mean J_z away from its initial value of zero. If we were concerned only with J_z then we could think of this shift as arising from the measurement starting to reveal the ‘true’ initial value of J_z , somewhere within the probability distribution for J_z with variance $J/2$. However, we know that this picture is not really true, because if J_z had a predefined value then J_x and J_y would be completely undefined, which is not the case with our state. In any case, the shift can be calculated to be

$$\begin{aligned} d\langle J_z \rangle_Y &= 2\sqrt{M} dW(t)(\Delta J_z)_Y^2 \\ &= 2\sqrt{M} Y(t) dt \langle J_z^2 \rangle_Y. \end{aligned} \quad (5.207)$$

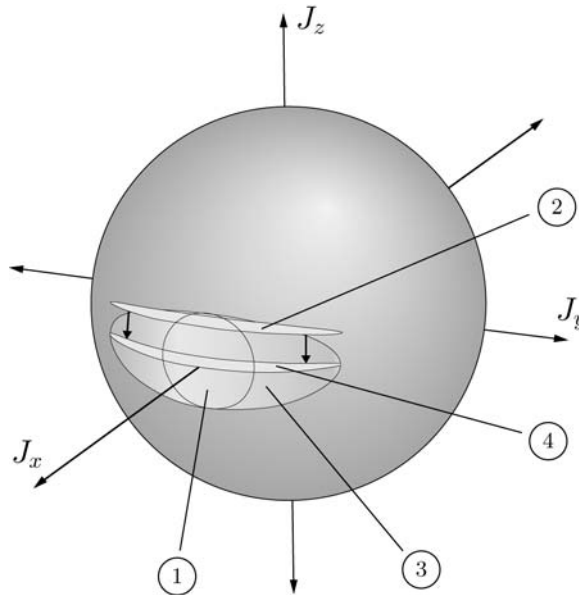


Fig. 5.4 Schematic quasiprobability distributions for the spin states, represented by ellipses on the Bloch sphere of radius J . The initial CSS, spin polarized in the x direction, is given by state 1. State 2 is one particular conditioned spin state after a measurement of J_z , while state 3 is the corresponding unconditioned state due to averaging over all possible conditioned states. The effect of the feedback is shown by state 4: a rotation about the y axis shifts the conditioned state 2 back to $\langle J_z \rangle_Y = 0$. The ensemble average of these conditioned states will then be similar to state 4. This is a reproduction of Fig. 2 of Ref. [TMW02a]. Based on Figure 2 from L. K. Thomsen *et al.*, Continuous Quantum Nondemolition Feedback and Unconditional Atomic Spin Squeezing, *Journal of Physics B: At. Mol. Opt. Phys.* **35**, 4937, (2002), IOP Publishing Ltd.

Exercise 5.37 Show this.

Hint: Initially $\langle J_z \rangle_Y = 0$ so that $Y(t) = dW/dt$.

Because the mean spin is initially in the x direction, a small shift in the mean J_z is equivalent to a small rotation of the mean spin about the y axis by an angle $d\phi \approx d\langle J_z \rangle_Y / J$. This is illustrated in Fig. 5.4, on a sphere. We call this the Bloch sphere, even though previously we have reserved this term for the $J = 1/2$ case.

Conditioning on the results of the measurement reduces the uncertainty in J_z below the SQL of $J/2$, while the deterministic term in the SME (5.204) increases the uncertainty in J_y . However, since the mean of J_z stochastically varies from zero (as shown in Eq. (5.207)), the atomic system conditioned on a particular measurement result is a squeezed spin state with just enough randomness in the direction of the mean spin to mask this spin-squeezing. The unconditioned system evolution $\dot{\rho} = M\mathcal{D}[\hat{J}_z]\rho$ is obtained by averaging over all the possible conditioned states, and this leads to a spin state with $(\Delta J_z)^2 = J/2$, the same as in a CSS. In other words, the squeezed character of individual conditioned system states is lost in the ensemble average. This is illustrated by the states 2 and 3 in Fig. 5.4.

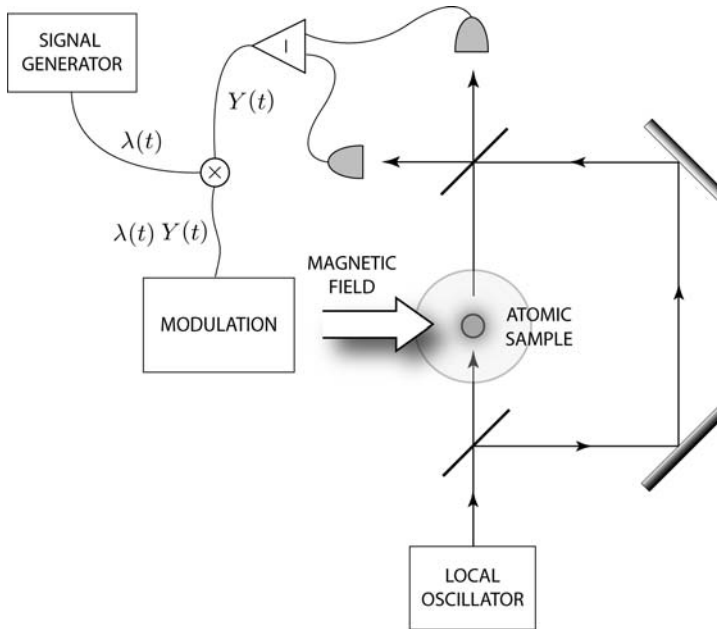


Fig. 5.5 A schematic diagram of an experimental apparatus that could be used for production of spin-squeezing via feedback. The laser probe passes through the ensemble of atoms and is detected by balanced homodyne detection. The current $Y(t)$ is fed back to control the magnetic field surrounding the atoms.

To retain the reduced fluctuations of J_z in the average evolution, we need a way of locking the conditioned mean spin direction. This can be achieved by feeding back the measurement results to drive the system continuously into the same squeezed state. The idea is to cancel out the stochastic shift of $\langle J_z \rangle_Y$ due to the measurement [TMW02b]. This simply requires a rotation of the mean spin about the y axis equal and opposite to that caused by Eq. (5.207). This is illustrated by state 4 in Fig. 5.4.

To make a rotation about the y axis proportional to the measured photocurrent $Y(t)$, we require a Hamiltonian of the form

$$\hat{H}_{\text{fb}}(t) = \lambda(t)Y(t)\hat{J}_y/\sqrt{M} = \hat{F}(t)Y(t), \quad (5.208)$$

where $\hat{F}(t) = \lambda(t)\hat{J}_y/\sqrt{M}$ and $\lambda(t)$ is the feedback strength. We have assumed instantaneous feedback because that is the form required to cancel out Eq. (5.207). Such a Hamiltonian can be effected by modulating the magnetic field in the region of the sample. This is shown in Fig. 5.5 from the experiment.

Assuming as above that $\langle J_z \rangle_Y = 0$, this feedback Hamiltonian leads to a shift in the mean J_z of

$$d\langle J_z \rangle_{\text{fb}} \approx -\lambda(t)Y(t)dt\langle J_x \rangle_Y/\sqrt{M}. \quad (5.209)$$

Since the idea is to produce $\langle J_z \rangle_Y = 0$ via the feedback, the approximations above and in Eq. (5.207) apply, and we can find a feedback strength such that Eq. (5.207) is cancelled out by Eq. (5.209). The required feedback strength for our scheme is thus

$$\lambda(t) = 2M\langle J_z^2 \rangle_Y / \langle J_x \rangle_Y. \quad (5.210)$$

This use of feedback to cancel out the noise in the conditional mean is the same technique as that which was found to be optimal in the linear system analysed in Section 5.6. The difference here is that the optimal feedback strength (5.210) depends upon conditional averages.

For experimental practicality it is desirable to replace the conditional averages in Eq. (5.210) by a predetermined function $\lambda(t)$ that could be stored in a signal generator. The evolution of the system including feedback can then be described by the master equation

$$\dot{\rho} = M\mathcal{D}[\hat{J}_z]\rho - i\lambda(t)[\hat{J}_y, \hat{J}_z\rho + \rho\hat{J}_z] + \frac{\lambda(t)^2}{M}\mathcal{D}[\hat{J}_y]\rho. \quad (5.211)$$

The choice of $\lambda(t)$ was considered in detail in Ref. [TMW02a], where it was shown that a suitable choice enables the master equation (5.211) to produce a Heisenberg-limited spin-squeezing ($\xi^2 \sim N^{-1}$) at a time $t \sim M^{-1}$.

5.7.3 Experimental considerations

For atoms in free space (as opposed to a cavity [NM08]), as discussed above and illustrated in Fig. 5.5, it is actually not possible to achieve Heisenberg-limited spin-squeezing by this method. This is because the decoherence time due to spontaneous emission is much shorter than the time $\sim M^{-1}$ required in order to attain the Heisenberg limit [TMW02a, NM08]. The relevant time-scale for a free-space configuration is in fact of order $(MN)^{-1}$, for which the degree of squeezing produced is moderate. In this limit it is possible to obtain a much simpler expression for the $\lambda(t)$ that should be used over the shorter time.

First note that the $\langle J_x \rangle_Y$ in Eq. (5.210) can be approximated by its initial value of J since the degree of squeezing is moderate. However, $\langle J_z^2 \rangle$ does change over this time, since this is precisely the squeezing we wish to produce. To find an expression for $\langle J_z^2 \rangle$, we assume that the atomic sample will approximately remain in a minimum-uncertainty state for J_z and J_y . This is equivalent to assuming that the feedback, apart from maintaining $\langle J_z \rangle = 0$, does not significantly alter the decreased variance of J_z that was produced by the measurement. This gives $\langle J_z^2 \rangle \approx J^2 / (4\langle J_y^2 \rangle)$, where we have again used $\langle J_x \rangle \approx J$. This procedure is essentially a linear approximation represented by replacing J_x by J in the commutator $[\hat{J}_y, \hat{J}_z] = i\hat{J}_x$. From the above master equation we obtain (under the same approximation) $\langle J_y^2 \rangle \approx J^2 Mt + J/2$.

Exercise 5.38 *Verify this.*

By substituting the approximation for $\langle J_y^2 \rangle$ into the expressions for $\langle J_x^2 \rangle$ we obtain

$$\lambda(t) \approx M(1 + NMt)^{-1}. \quad (5.212)$$

With this choice, a squeezing of

$$\xi^2(t) \approx (1 + NMt)^{-1} \quad (5.213)$$

will be produced at time t , and this will be valid as long as $Mt \ll 1$. Spontaneous emission, and other imperfections, are of course still being ignored.

Exercise 5.39 Show that, if λ is held fixed, rather than varied, the variance for the conditioned mean $\langle J_z \rangle_Y$ at time t is

$$[e^{-4\lambda Jt} - (1 + 2JMt)^{-1}] \frac{J}{2} + (1 - e^{-4\lambda Jt}) \frac{\lambda J}{4M}. \quad (5.214)$$

Hint: Remember that for linear systems $\langle J_z^2 \rangle = \langle J_z^2 \rangle_Y + \langle J_z \rangle_Y^2$.

An experiment along the lines described above (with λ fixed) has been performed, with results that appeared to reflect moderate spin-squeezing [GSM04]. Unfortunately the published results were not reproducible and exhibited some critical calibration inconsistencies. The authors have since concluded that they must have been spurious and have retracted the paper [GSM08], saying that ‘analyzing Faraday spectroscopy of alkali clouds at high optical depth in precise quantitative detail is surprisingly challenging’. High optical depth leads to significant difficulties with the accurate determination of effective atom number and degree of polarization (and thus of the CSS uncertainty level), while technical noise stemming from background magnetic fields and probe polarization or pointing fluctuations can easily mask the atomic spin projection signal. An additional complication relative to the simple theory given above is that the experiment was performed by probing cesium atoms on an optical transition with many coupled hyperfine-Zeeman states, rather than the two levels considered above. There is still a linear coupling of the probe field to the angular-momentum operator \hat{j}_z defined on the entire hyperfine-Zeeman manifold, which can in principle be utilized to generate measurement-induced spin-squeezing. However, there is also a nonlinear atom–probe interaction that can corrupt the Faraday-rotation signals if it is not suppressed by very careful probe-polarization alignment. For more details see Ref. [Sto06]. Continuing research has led to the development of technical noise-suppression techniques and new modelling and calibration methods that enable accurate high-confidence determination of the CSS uncertainty level [MCSM], providing hope for improved experimental results regarding the measurement and control of spin-squeezing in the future.

5.8 Further reading

5.8.1 Coherent quantum feedback

It was emphasized in Section 5.2 that even when we use an operator to describe the feedback current, as is necessary in the Heisenberg picture, we do not mean to imply that the feedback apparatus is truly quantum mechanical. That is, the feedback Hamiltonians we

use are model Hamiltonians that produce the correct evolution. They are not to be taken seriously as dynamical Hamiltonians for the feedback apparatus.

However, there are situations in which we might wish to consider a very small apparatus, and to treat it seriously as a quantum system, with no classical measurement device taking part in the dynamics. We could still consider this to be a form of quantum feedback if the Hamiltonian for the system of interest S and apparatus A were such that the following applied.

1. S and A evolve for time t_m under a joint Hamiltonian \hat{H}_{coup} .
2. S and A may then evolve independently.
3. S and A then evolve for time t_c under another joint Hamiltonian $\hat{H}_{\text{fb}} = \hat{F}_S \otimes \hat{J}_A$.

The form of \hat{H}_{fb} ensures that, insofar as S is concerned, the dynamics could have been implemented by replacing step 3 by the following two steps.

3. The apparatus observable \hat{J}_A is measured yielding result J .
4. S then evolves for time t_c under the Hamiltonian $\hat{H}_{\text{fb}} = \hat{F}_S \times J$.

That is, the feedback could have been implemented classically.

Lloyd has called feedback of this sort (without measurement) *coherent quantum feedback* [Llo00], and it was demonstrated experimentally [NWCL00] using NMR quantum information-processing techniques. Previously, this concept was introduced in a quantum-optics context as *all-optical feedback* (as opposed to electro-optical feedback) [WM94b]. An important feature of coherent feedback is that, although on average the evolution of system S is the same as for measurement-based feedback, it would be possible to measure the apparatus A (after the action of \hat{H}_{fb}) in a basis in which \hat{H}_{fb} is not diagonal. This would produce conditional states of system S incompatible with the conditional states of measurement-based feedback, in which \hat{J} really was measured.

Exercise 5.40 *Convince yourself of this.*

We will consider an example of ‘coherent’ quantum feedback in Section 7.7.

An even more general concept of quantum feedback is to drop the above constraints on the system–apparatus coupling, but still to engineer the quantum apparatus so as to achieve some goal regarding the system state or dynamics. Examples of this from all-optical feedback were considered in Ref. [WM94b], and there has recently been renewed interest in this area [Mab08]. This concept is so general that it encompasses any sort of engineered interaction between quantum systems. However, under some circumstances, ideas from engineering control theory naturally generalize to the fully quantum situation, in which case it is sensible to consider this to be an aspect of quantum control. For details see Ref. [Mab08] and references contained therein.

5.8.2 Other applications of quantum feedback

There are many other instances for the application of Markovian quantum feedback besides those mentioned in this chapter. Here are a few of them.

Back-action elimination. Recall from Section 1.4.2 that, for efficient measurements, any measurement can be considered as a minimally disturbing measurement followed by unitary evolution that depends on the result. This leads naturally to the idea, proposed in Ref. [Wis95], of using feedback to eliminate this unnecessary unitary back-action. A quantum-optical realization of a QND measurement of a quadrature using this technique was also proposed there. Courty, Heidman and Pinard [CHP03] have proposed using this principle to eliminate the radiation-pressure back-action in the interferometric measurement of mirror position. Their work has important implications for gravitational-wave detection.

Decoherence control. The Horoshko–Kilin scheme (see Section 5.4.3) for protecting a Schrödinger cat from decoherence due to photon loss works only if the lost photons are detected (and the information fed back). In the microwave regime lost photons cannot in practice be detected, so an alternative approach is necessary. Several feedback schemes have been suggested – see Ref. [ZVTR03] and references therein. In Ref. [ZVTR03], Zippilli *et al.* showed that the parity of the microwave cat state can be probed by passing an atom through the cavity. The same atom, containing the result of the ‘measurement’, can then be used to implement feedback on the mode during the latter part of its passage through the cavity. This is thus an example of the coherent feedback discussed above. They showed that the lifetime of the cat state can, in principle, be arbitrarily enhanced by this technique.

Engineering invariant attractive subsystems. The preparation of a two-level quantum system in a particular state by Markovian feedback was considered in Refs. [HHM98, WW01, WWM01] (see also Section 6.7.2). A much more general approach is discussed in Ref. [TV08], namely engineering attractive and invariant dynamics for a subsystem. Technically, a subsystem is a system with Hilbert space \mathbb{H}_S such that the total Hilbert space can be written as $(\mathbb{H}_S \otimes \mathbb{H}_F) \oplus \mathbb{H}_R$. Attractive and invariant dynamics for the subsystem means that in the long-time limit the projection of the state onto \mathbb{H}_R is zero, while the state on $\mathbb{H}_S \otimes \mathbb{H}_F$ has the form $\rho_S \otimes \rho_F$, for a particular ρ_S . Ticozzi and Viola discuss the conditions under which such dynamics can be engineered using Markovian feedback, for a given measurement interaction and Markovian decoherence. This is potentially useful for preparing systems for quantum information processing (see Chapter 7).

Linewidth narrowing of an atom laser. A continuous atom laser consists of a mode of bosonic atoms continuously damped, so as to form a beam, and continuously replenished. Such a device, which has yet to be realized, will almost certainly have a spectral linewidth dominated by the effect of the atomic interaction energy, which turns fluctuations in the condensate atom number into fluctuations in the condensate frequency. These correlated fluctuations mean that information about the atom number could be used to reduce the frequency fluctuations, by controlling a spatially uniform potential. Obtaining information about the atom number by a quantum-non-demolition measurement (similar to that discussed in Section 5.7) is a process that itself causes phase fluctuations, due to measurement back-action. Nevertheless, it has been shown that Markovian feedback based upon such a measurement could reduce the linewidth by many orders of magnitude [WT01, TW02].

Cooling of a trapped ion (theory and experiment). The motion of a single ion in a Paul trap [WPW99] can be treated as a harmonic oscillator. By using its internal electronic states and coupling to external lasers, it can be cooled using so-called Doppler cooling [WPW99]. However, the equilibrium thermal occupation number (the number of phonons of motion) is still large. It was shown by Steixner, Rabl and Zoller [SRZ05] that in this process some of the light emitted from the atom can be detected in a manner that allows a measurement of one quadrature of the ion's motion (similar to homodyne detection of an optical field). They then show, using Markovian feedback theory as presented here, that the measured current can be fed back to the trap electrodes to cool the motion of the ion. Moreover, this theory has since been verified experimentally by the group of Blatt [BRW⁺06], demonstrating cooling by more than 30% below the Doppler limit.

Linewidth narrowing of an atom by squashed light. It has been known for some time [Gar86] that a two-level atom strongly coupled to a beam of broad-band squeezed light will have the decay rate of one of its dipole quadratures changed by an amount proportional to the normally ordered spectrum of squeezing (i.e. the decay rate will be reduced). This could be seen by observing a narrow feature in the power spectrum of the emission of the atom into the non-squeezed modes to which it is coupled. It was shown in Ref. [Wis98] that the same phenomenon occurs for a squashed beam (see Section 5.2.5) as produced by a feedback loop. Note that an atom is a nonlinear optical element, so that a semiclassical theory of squashing cannot explain this effect, which has yet to be observed.

Applications of quantum feedback control in quantum information will be considered in Chapter 7.